

SINGULARITIES OF THREE-DIMENSIONAL BILLIARDS BOUNDED BY CONFOCAL QUADRICS

Gleb Belozеров and Anatoly Fomenko

ABSTRACT. The problem of motion of a material point in a three-dimensional domain bounded by confocal quadrics is considered. Such a dynamical system is Liouville integrable in the piecewise-smooth sense. For two types of billiard regions, the regions of possible motion of a material point are found, the bifurcation diagrams are constructed, and the semi-local structure of the Liouville foliation is described. On singular Liouville foliation layers of nonzero rank, at least one action variable can be smoothly extended. This consideration, applied to the billiard inside a three-axial ellipsoid, gave a new proof of Staude's construction of an ellipsoid using a thread.

1. Introduction

Currently, integrable Hamiltonian systems (hereinafter referred to as IHS), their topological and trajectory characteristics are actively studied. The most geometrically visual IHS are integrable billiards and their generalisations.

The integrability of the plane billiard in the region bounded by an ellipse is noted in the work of J. D. Birkhoff [1]. In the book by V. V. Kozlov and D. V. Treshchev [2], as well as in the book by S. L. Tabachnikov [3], a review of modern and classical studies devoted to the theory of mathematical billiards is given.

The plane billiards inside regions bounded by arcs of confocal quadrics are also integrable. Such systems have been studied up to the Liouville equivalence in the works of V. Dragovich, M. Radnovich [4, 5], and V. V. Vedyushkina [6, 7].

V. V. Vedyushkina introduced and considered a new class of integrable billiards - billiards on table books i.e., CW -complexes glued from elementary plane confocal regions along some common (isometric) parts of the boundaries. Each edge of the gluing is assigned a permutation that determines the dynamics of a material point falling on the edge. The billiards on table-books realise Liouville foliations of many important IHSs. Moreover, according to the results of V. V. Vedyushkina and I. S. Kharcheva, billiard books model all three-dimensional bifurcations of IHSs

2020 *Mathematics Subject Classification:* 37J20.

Key words and phrases: integrable Hamiltonian system, integrable billiard, Liouville foliation, confocal quadrics, Staude's construction.

(see [8]), and also realise the Liouville bases of all IHSs of two degrees of freedom on compact surfaces of constant energy (see [9]).

In addition to billiard books, there are other integrable generalisations of the classical billiard inside an ellipse. These include billiards with integrable potentials [10–13], confocal billiards on the Minkowski plane [14, 15], billiards with slipping [16], evolutionary force billiards [17, 18], and confocal geodesic billiards on quadrics [19].

The study of the topology of the Liouville foliation in most of these papers is reduced to the calculation of topological invariants. The method of invariants for the qualitative analysis of IHSs was introduced by A. T. Fomenko (see [20]–[23]).

The present paper is devoted to the study of the Liouville foliation topology of three-dimensional billiards bounded by confocal quadrics. Such billiards are Liouville integrable in the piecewise-smooth sense. We will prove this fact in the third section.

Regular Liouville foliation layers of the billiard inside a three-axial ellipsoid and their 1-bifurcations were described by V. Dragovich and M. Radnovich in [5]. In [24] G. V. BelozeroV classified all three-dimensional billiard regions bounded by confocal quadrics (assuming that all dihedral angles of the boundary break are equal to $\pi/2$) with respect to their combinatorial structure, described the regular layers of the corresponding billiards and their 1-bifurcations, and defined the homeomorphism classes of the constant energy surfaces.

In the present paper, for two types of billiard regions (namely, the region inside an ellipsoid and the region bounded by an ellipsoid and a sheet of a confocal two-sheet hyperboloid), the regions of position motion are defined, the bifurcation diagrams are constructed, and the structure of Liouville foliation near all singular layers is described.

It is well known that an ellipse can be drawn by two points (foci) using a thread. Moreover, if we take an ellipse, throw a thread over it, stretch the thread to the limit and draw the curve, the result will be an ellipse confocal with the given one. This fact was discovered by the British bishop Ch. Graves in 1851. Recently, it was discovered by the authors when studying the trajectory properties of integrable billiards (see [25]). As it turned out, this result is easy to prove by using action variables of the billiard inside an ellipse. We were able to apply the reasoning with action variables to the three-dimensional case and to prove the Staude’s construction of a three-axial ellipsoid by using a thread (see about this construction [26]).

2. Confocal quadrics in \mathbb{R}^3 and their properties

DEFINITION 2.1. A family of confocal quadrics in three-dimensional Euclidean space $\mathbb{R}^3(x, y, z)$ is the set of quadrics given by the equation

$$(2.1) \quad (b - \lambda)(c - \lambda)x^2 + (a - \lambda)(c - \lambda)y^2 + (a - \lambda)(b - \lambda)z^2 = (a - \lambda)(b - \lambda)(c - \lambda),$$

where $a > b > c$ are fixed numbers and λ is a real parameter. If the parameter of a quadric of this family is equal to a , b or c , the quadric is called *degenerate*, otherwise it is called *non-degenerate*.

REMARK 2.1. Degenerate quadrics are coordinate planes. If $\lambda \in (-\infty, c)$, then the corresponding quadric is an ellipsoid; if $\lambda \in (c, b)$, then the quadric is a one-sheet hyperboloid, if $\lambda \in (b, a)$, then the quadric is a two-sheet hyperboloid. Figure 1 shows three confocal quadrics in \mathbb{R}^3 of different types.

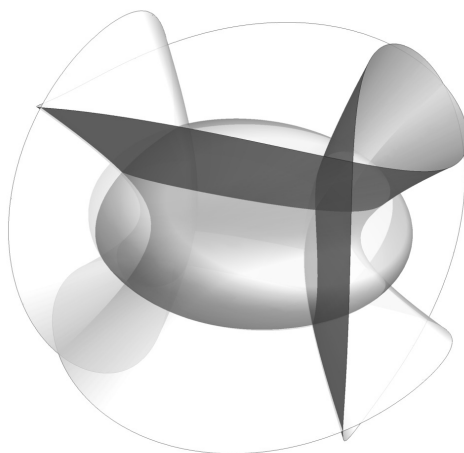


FIGURE 1. Three confocal quadrics in \mathbb{R}^3 : an ellipsoid, an one-sheet hyperboloid, a two-sheet hyperboloid.

REMARK 2.2. In the Euclidean n -dimensional space $\mathbb{R}^n(x_1, \dots, x_n)$ a family of confocal quadrics is defined by the formula

$$\frac{x_1^2}{a_1 - \lambda} + \dots + \frac{x_n^2}{a_n - \lambda} = 1,$$

where $a_1 > \dots > a_n$ are constant numbers and λ is a real parameter. The following facts about confocal quadrics in \mathbb{R}^3 can be easily generalised to the case of an arbitrary dimension.

REMARK 2.3. Confocal quadrics and their properties were studied by K. Jacobi in [28], and by M. Chasles in [29]. These properties are the basis of the proof of the famous Jacobi-Chasles theorem on the integrability of the geodesic flow on ellipsoids in \mathbb{R}^n .

The family of confocal quadrics has a lot of remarkable properties. All these properties are well known. The reader can find them, for example, in the works of K. Jacobi [28] and V. I. Arnold [30]. However, for the sake of completeness, we will recall a few of them.

PROPOSITION 2.1. *The tangent planes at the intersection points of two confocal quadrics are orthogonal.*

PROOF. Let us prove the proposition for non-degenerate quadrics of parameters λ_1 and λ_2 . In this case, the equations 2.1 of these quadrics can be divided by the

corresponding expressions $(a-\lambda_i)(b-\lambda_i)(c-\lambda_i)$. The coordinates of the intersection points of the quadrics satisfy the following system:

$$\begin{cases} \frac{x^2}{a-\lambda_1} + \frac{y^2}{b-\lambda_1} + \frac{z^2}{c-\lambda_1} = 1 \\ \frac{x^2}{a-\lambda_2} + \frac{y^2}{b-\lambda_2} + \frac{z^2}{c-\lambda_2} = 1 \end{cases}$$

Subtract the second equation from the first equation, and then, divide the resulting expression by $\lambda_1 - \lambda_2$:

$$\frac{x^2}{(a-\lambda_1)(a-\lambda_2)} + \frac{y^2}{(b-\lambda_1)(b-\lambda_2)} + \frac{z^2}{(c-\lambda_1)(c-\lambda_2)} = 0.$$

Since the left part of the last expression is the scalar product of the gradients of the functions defining the quadrics, this equation can be reformulated as follows: the vectors of normals at the intersection points of two confocal quadrics are orthogonal. But this is equivalent to the statement to be proved. The proposition is proved. \square

PROPOSITION 2.2. *Through each point $P = (x, y, z) \in \mathbb{R}^3$ such that $x \neq 0$, $y \neq 0$, $z \neq 0$, there pass exactly three non-degenerate confocal quadrics: an ellipsoid, an one-sheet hyperboloid, and a two-sheet hyperboloid.*

PROOF. For a point P , all of whose Cartesian coordinates are nonzero, consider the function $f_P(\lambda) = \frac{x^2}{a-\lambda} + \frac{y^2}{b-\lambda} + \frac{z^2}{c-\lambda}$. Note that $\lim_{\lambda \rightarrow -\infty} f(\lambda) = 0$ and for $k = a, b, c$ we have $\lim_{\lambda \rightarrow k-0} f(\lambda) = +\infty$, $\lim_{\lambda \rightarrow k+0} f(\lambda) = -\infty$. From this, as well as from the Weierstrass theorem on the intermediate value of a continuous function, we conclude that on the intervals $(-\infty, c)$, (c, b) , (b, a) the roots of the equation $f_P(\lambda) = 1$ must necessarily be found (see Fig. 2).

Thus, three confocal quadrics necessarily pass through the point P : an ellipsoid and two hyperboloids. To prove that there are no more than three roots, it suffices to show that the function $f_P(\lambda)$ is increasing on the intervals $(-\infty, c)$, (c, b) , (b, a) .

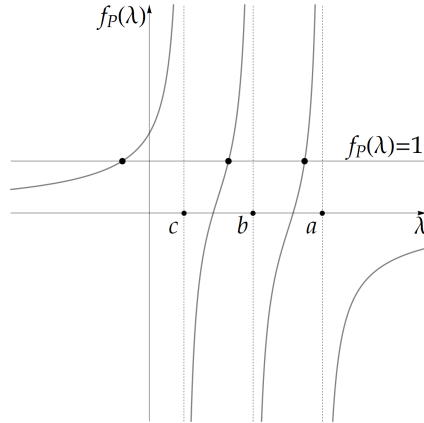


FIGURE 2. An illustration of the fact that the equation $f_P(\lambda) = 1$ has exactly three real roots.

This can be easily verified by calculating the derivative of $f_P(\lambda)$. The proposition is proved. \square

PROPOSITION 2.3. *Through each point \mathbb{R}^3 there pass three confocal quadrics, taking into account the multiplicity. If we sort the parameters of these quadrics in ascending order and denote them by $\lambda_1 \leq \lambda_2 \leq \lambda_3$, then $\lambda_1 \in (-\infty, c]$, $\lambda_2 \in [c, b]$, $\lambda_3 \in [b, a]$.*

PROOF. Note that the parameters of the confocal quadrics passing through the point $P = (x, y, z)$ are the roots of the cubic equation 2.1. According to Proposition 2.2, at each point inside any coordinate octant, this equation has exactly three real roots. Since the coefficients of equation 2.1 smoothly depend on the Cartesian coordinates of the point P , and the planes Oxy , Oxz , Oyz are sets of measure zero, this equation has three real roots at an arbitrary point of \mathbb{R}^3 . The restrictions on the ranges of these roots also follow from Proposition 2.2. The proposition is proved. \square

Let $P \in \mathbb{R}^3$, and $\lambda_1 \leq \lambda_2 \leq \lambda_3$ are the parameters of confocal quadrics passing through P .

DEFINITION 2.2. The functions $\lambda_1, \lambda_2, \lambda_3$ are called *elliptic coordinates* in \mathbb{R}^3 .

PROPOSITION 2.4. *The relations between elliptic and Cartesian coordinates are described by the following system:*

$$(2.2) \quad \begin{cases} x^2 = \frac{(a-\lambda_1)(a-\lambda_2)(a-\lambda_3)}{(a-b)(a-c)} \\ y^2 = \frac{(b-\lambda_1)(b-\lambda_2)(b-\lambda_3)}{(b-a)(b-c)} \\ z^2 = \frac{(c-\lambda_1)(c-\lambda_2)(c-\lambda_3)}{(c-a)(c-b)} \end{cases}$$

PROOF. Verified by direct calculations. \square

Using the last proposition, it is easy to show that, in each coordinate octant, the elliptic coordinates are single-valued, smooth and regular.

For further analysis it is necessary to find out how those points where some of the elliptic coordinates coincide are structured. It is well known that on the plane such points are the foci of a family of confocal quadrics. In our case, there are two possible options: $\lambda_1 = \lambda_2 = c$, $\lambda_2 = \lambda_3 = b$. Let's consider each of them.

1. $\lambda_1 = \lambda_2 = c$. Let us use the formulae 2.2. From the third equation, we conclude that all such points lie in the plane $z = 0$. Let us substitute $\lambda_1 = \lambda_2 = c$ into the first and second equations of the system 2.2.

$$\begin{cases} x^2 = \frac{a-c}{a-b}(a-\lambda_3) \\ y^2 = \frac{b-c}{b-a}(b-\lambda_3) \end{cases}$$

Let us express λ_3 from these equations, and then equate the resulting expressions:

$$\frac{x^2}{a-c} + \frac{y^2}{b-c} = 1.$$

The last equation defines the ellipse \mathfrak{F}_1 lying in the plane $z = 0$.

2. $\lambda_2 = \lambda_3 = b$. Similar reasoning shows that all such points are located in the plane $y = 0$ on the hyperbola \mathfrak{F}_2 given by the equation

$$\frac{x^2}{a-b} - \frac{z^2}{b-c} = 1.$$

DEFINITION 2.3. The ellipse \mathfrak{F}_1 and the hyperbola \mathfrak{F}_2 are called *focal curves*.

Let us list some properties of focal curves.

PROPOSITION 2.5. *The ellipse \mathfrak{F}_1 consists of all ombilic points of two-sheet hyperboloids of a given family of confocal quadrics, and the hyperbola \mathfrak{F}_2 consists of all ombilic points of ellipsoids of the same family.*

PROOF. It is known that an ellipsoid of the form $\frac{x^2}{\alpha^2} + \frac{y^2}{\beta^2} + \frac{z^2}{\gamma^2} = 1$, where $\alpha > \beta > \gamma > 0$, has exactly 4 ombilic points whose coordinates satisfy the relations: $x^2 = \alpha^2 \frac{\alpha^2 - \beta^2}{\alpha^2 - \gamma^2}$, $y = 0$, $z^2 = \gamma^2 \frac{\beta^2 - \gamma^2}{\alpha^2 - \gamma^2}$.

In our case, $\alpha^2 = a - \lambda$, $\beta^2 = b - \lambda$, $\gamma^2 = c - \lambda$. Let us substitute these expressions into the equations of ombilic points: $x^2 = (a - \lambda) \frac{a-b}{a-c}$, $y = 0$, $z^2 = (c - \lambda) \frac{b-c}{a-c}$. Divide the first equation by $\frac{a-c}{a-b}$, and divide the third equation by $-\frac{a-c}{b-c}$, then add them up:

$$x^2 \frac{a-c}{a-b} - z^2 \frac{a-c}{b-c} = a-c.$$

Dividing the last equality by $a-c$, we obtain the equation of the hyperbola \mathfrak{F}_2 . Similarly, it can be shown that the ellipse \mathfrak{F}_1 consists of ombilic points of two-sheet hyperboloids of the family. The proposition is proved. \square

PROPOSITION 2.6. *The ellipse \mathfrak{F}_1 passes through the foci of the hyperbola \mathfrak{F}_2 , and the hyperbola \mathfrak{F}_2 passes through the foci of the ellipse \mathfrak{F}_1 .*

PROOF. Verified by direct calculations. \square

Note that in the planar case, the location of the foci has uniquely defined a family of confocal quadrics. However, is there an analogue of such points for confocal families in \mathbb{R}^3 ? Yes, in fact, there is. Note that the curves \mathfrak{F}_1 and \mathfrak{F}_2 (by themselves) uniquely reconstruct the family of confocal quadrics in \mathbb{R}^3 , since their semi-axes contain information about the values $a-b, a-c$. Thus, according to the Proposition 2.6, we can reconstruct the ellipse \mathfrak{F}_1 and the hyperbola \mathfrak{F}_2 if we know the location of their foci (to the precision of rotation around the focal line). Thus, based on the foci of the curves \mathfrak{F}_1 and \mathfrak{F}_2 , we can reconstruct the family of confocal quadrics (see Fig. 3). So, these four points can be considered as *foci* of the family of confocal quadrics in \mathbb{R}^3 . Note that the focal points of families of focal quadrics in an arbitrary Euclidean \mathbb{R}^n were introduced in the works of V. Dragovich and B. Gajich [31]- [32].

It is well known that an ellipse can be drawn using a thread. If you fix the two ends of a thread at two fixed points, stretch it with a pencil to the limit, and then draw a line (leaving the thread taut), the result will be an ellipse. The foci of the ellipse are the fixed ends of the thread.

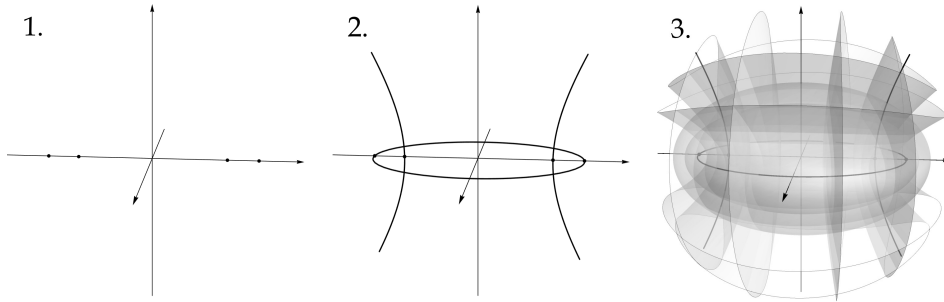


FIGURE 3. Reconstruction of the family of confocal quadrics from two pairs of points symmetrically located on the axis Ox . We first determine the focal curves (transition from 1 to 2), and then find the family of confocal quadrics (transition from 2 to 3).

It turns out that an ellipsoid in three-dimensional Euclidean space can be constructed by a similar way. Let \mathfrak{F}_1 and \mathfrak{F}_2 be the focal ellipse and hyperbola of some family of confocal quadrics in \mathbb{R}^3 , and let F and G be the foci of \mathfrak{F}_2 and \mathfrak{F}_1 lying on opposite sides of the plane $x = 0$. Let us locate the movable joints P_2 and P_1 on the focal ellipse \mathfrak{F}_1 and the branch of the hyperbola \mathfrak{F}_2 not containing the point G , respectively. Pass one end of the thread through P_1 and fix it at F , and pass the other end through P_2 and fix it at G . Let us stretch the thread to its limit at point P , located on the section of thread between the joints. It turns out that point P will move along the surface of an ellipsoid confocal with \mathfrak{F}_1 and \mathfrak{F}_2 (see Fig. 4). Moreover, it will cover its quarter. Note that in the stretched position of the thread, the lines PP_1 and PP_2 pass through both focal curves.

This construction was introduced by Staude in 1882. As it turned out, it is closely related to the integrability of the billiard inside an ellipsoid (namely, with the action variables) and can be generalised to the case of an arbitrary dimension. In the final section, we give a brief proof of the construction.

3. Confocal Billiards. Integrability

3.1. Description of the system. Let us fix a family of confocal quadrics in \mathbb{R}^3 .

DEFINITION 3.1. A *three-dimensional billiard table* \mathcal{Z}^3 is the closure of a connected bounded region in \mathbb{R}^3 whose boundary consists of a finite number of smooth faces lying on quadrics of a confocal family. Also, we will assume that the dihedral break angles at the boundary of \mathcal{Z}^3 are equal to $\pi/2$.

REMARK 3.1. Such regions in \mathbb{R}^k for arbitrary k arose in the paper [33] of V. Dragovich and M. Radnovich, in which they studied trajectory properties of the corresponding billiard systems.

Figure 5 shows two three-dimensional billiard tables.

Let \mathcal{Z}^3 be a three-dimensional billiard table. Consider the following dynamical system: a material point of unit mass moves inside \mathcal{Z}^3 along straight lines with

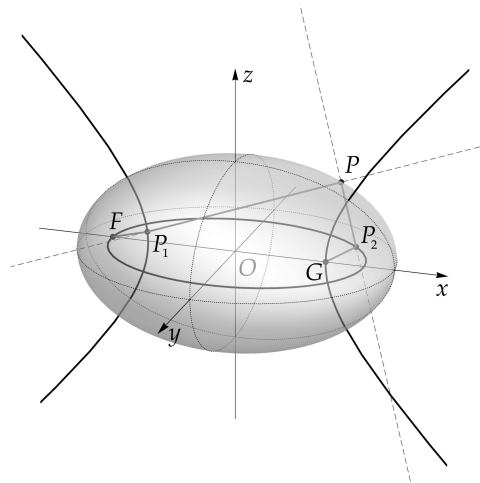


FIGURE 4. Focal property of an ellipsoid in \mathbb{R}^3 : the sum of $FP_1 + P_1P + PP_2 + P_2G$ is constant.

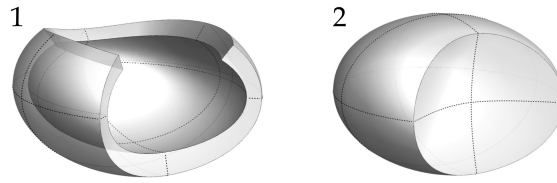


FIGURE 5. Examples of three-dimensional billiard tables. Dotted lines indicate the areas of intersection of tables with coordinate planes.

constant velocity, reflecting from the boundary of the table absolutely elastically. We will call such a dynamical system *three-dimensional confocal billiard*.

It remains to determine the dynamics of the material point at the break points of the billiard table boundary. Since all dihedral break angles at the \mathcal{Z}^3 boundary are equal to $\pi/2$, the reflection at such points can be further defined by continuity. Namely, when hitting point x of the \mathcal{Z}^3 boundary, the particle's velocity vector must be reflected sequentially from all walls of the table that meet at x .

REMARK 3.2. Due to the elliptic coordinates orthogonality, the reflections from the walls of the billiard table \mathcal{Z} commute with each other. Therefore, the result of the reflection of vector v does not depend on the sequence of its reflections from the tangent planes of the quadrics that are part of the table boundary at point x . It is also important for us that all the break angles at the table boundary are equal to $\pi/2$, and not $3\pi/2$, since this property allows us to uniquely determine the reflection at the break points by continuity.

The phase space of three-dimensional confocal billiards is a factor set $M^6 = \{(x, v) | x \in \mathcal{Z}^3, v \in T_x\mathbb{R}^3 - 0\} / \sim$ with the factor topology, where \sim is the following equivalence relation on the boundary of the table \mathcal{Z}^3 . Pairs (x_1, v_1) and (x_2, v_2) , where $x_1, x_2 \in \partial\mathcal{Z}^3$, are *equivalent* if and only if $x_1 = x_2$ and the vector v_2 can be obtained from v_1 by several consecutive reflections relative to the walls of \mathcal{Z}^3 , which meet at this point.

Note that the function $H = \frac{1}{2}(\dot{x}^2 + \dot{y}^2 + \dot{z}^2)$ is a first integral of a three-dimensional confocal billiard. It is continuous on M^6 .

Due to reflection, the phase space M^6 of the considered system, in general, is not a smooth manifold. Nevertheless, for all values $h > 0$ the isoenergetic surface $Q_h^5 = \{(x, v) \in M^6 | H(x, v) = h\}$ is a topological manifold. The proof of this fact is given in [27]. It turns out that the isoenergetic surface of a three-dimensional confocal billiard is homeomorphic to either a five-dimensional sphere, i.e., S^5 , or to the direct product of a circle and a four-dimensional sphere, i.e., $S^1 \times S^4$, or to the direct product of a two-dimensional sphere and a three-dimensional sphere, i.e., $S^2 \times S^3$.

3.2. System integrability. Let us denote by \widetilde{M}^6 the union of smooth parts of the phase space of the three-dimensional confocal billiard inside a table \mathcal{Z}^3 . Let us make a number of observations.

- (1) On \widetilde{M}^6 the non-degenerate closed 2-form $\omega = dx \wedge dv_1 + dy \wedge dv_2 + dz \wedge dv_3$ is correctly defined, where v_1, v_2, v_3 are the coordinates of the velocity vector of a material point in the basis $\partial/\partial x, \partial/\partial y, \partial/\partial z$.
- (2) The dynamics of a point on the manifold \widetilde{M}^6 is determined by the vector field $\text{sgrad } H = \omega^{-1} \nabla H$.
- (3) There exist continuous limits of the form ω “from the right” and “from the left” as we tend to the region of non-smoothness M^6 (i.e. in all pairs $(x, v) \in M^6$, where $x \in \partial\mathcal{Z}^3$).

The function H , as in the smooth case, will be called the *Hamilton function* (*Hamiltonian*).

For dynamic systems with properties (1) — (3), A. T. Fomenko introduced the notion of Liouville integrability in the piecewise-smooth sense. Let us recall its definition.

DEFINITION 3.2. We will say that the dynamical system defined by the Hamilton function H is *integrable by Liouville in the piecewise-smooth sense* if there exist continuous on M^6 and smooth on \widetilde{M}^6 first integrals F_1, F_2 such that:

- (1) H, F_1, F_2 are functionally independent, i.e. their gradients are almost everywhere linearly independent on \widetilde{M}^6 ;
- (2) H, F_1, F_2 commute on \widetilde{M}^6 with respect to the Poisson bracket defined by the form ω .

It turns out that three-dimensional confocal billiards are integrable by Liouville in the piecewise-smooth sense. This fact for some billiard tables (for example, for the region bounded by an ellipsoid) follows from Jacobi’s theorem on the integrability of the geodesic flow on the surface of an ellipsoid (see [28, 34–36]).

Nevertheless, we will give a proof of this result for an arbitrary three-dimensional confocal billiard.

THEOREM 3.1. *Three-dimensional billiards bounded by confocal quadrics are integrable by Liouville in a piecewise-smooth sense. Moreover, all segments of an arbitrary trajectory-break (or their extensions) of a material point of a three-dimensional confocal billiard are tangent to two confocal quadrics (taking into account multiplicity) common to all parts of the trajectory.*

PROOF. Consider the motion of a material point of unit mass by inertia in \mathbb{R}^3 . Let us define the parameters of the quadrics of a confocal family 2.1, which are touched by the line-trajectory of the material point. Let at some moment of time the particle be at the point $P = (x, y, z)$ with velocity vector $v = (\dot{x}, \dot{y}, \dot{z})$. The parametrization of its trajectory has the form: $P + \tau v, \tau \in \mathbb{R}$. Let us substitute it into the equation of the confocal family. We obtain a quadratic equation with respect to τ . Hence we conclude that the trajectory touches the confocal quadric of the parameter λ if and only if the discriminant of this quadratic equation is zero, which is equivalent to the following equality.

$$(3.1) \quad \left(\frac{x\dot{x}}{a-\lambda} + \frac{y\dot{y}}{b-\lambda} + \frac{z\dot{z}}{c-\lambda} \right)^2 = \left(\frac{\dot{x}^2}{a-\lambda} + \frac{\dot{y}^2}{b-\lambda} + \frac{\dot{z}^2}{c-\lambda} \right) \cdot \left(\frac{x^2}{a-\lambda} + \frac{y^2}{b-\lambda} + \frac{z^2}{c-\lambda} - 1 \right).$$

The roots λ of this equation are the parameters of the tangent quadrics.

We transform the equation 3.1 by multiplying it by $(a-\lambda)(b-\lambda)(c-\lambda)$. As a result, we obtain a quadratic equation with respect to λ : $H\lambda^2 - F_1\lambda + F_2 = 0$, where H is the (kinetic) energy of a material point, and the functions F_1 and F_2 are calculated by the formulae:

$$F_1 = \frac{1}{2}((b+c)\dot{x}^2 + (a+c)\dot{y}^2 + (a+b)\dot{z}^2) - \frac{1}{2}(K_x^2 + K_y^2 + K_z^2),$$

$$F_2 = \frac{1}{2}(bc\dot{x}^2 + ac\dot{y}^2 + ab\dot{z}^2) - \frac{1}{2}(aK_x^2 + bK_y^2 + cK_z^2).$$

Here K_x, K_y, K_z are the components of the kinetic momentum vector K of the material point. Recall that $K = P \times v$. Let us call the trinomial $H\lambda^2 - F_1\lambda + F_2$ the *tangent polynomial*.

Since the functions H, F_1, F_2 are polynomial, it is easy to compute their pairwise Poisson brackets and verify that they are all zero. However, in order to analyse the deeper meaning of these functions, let us pass to the elliptic coordinates $\lambda_1, \lambda_2, \lambda_3$ and their conjugate momenta p_1, p_2, p_3 . We obtain that

$$H = 2 \left(\frac{\Delta_1}{(\lambda_1 - \lambda_2)(\lambda_1 - \lambda_3)} p_1^2 + \frac{\Delta_2}{(\lambda_2 - \lambda_1)(\lambda_2 - \lambda_3)} p_2^2 + \frac{\Delta_3}{(\lambda_3 - \lambda_1)(\lambda_3 - \lambda_2)} p_3^2 \right),$$

$$F_1 = 2 \left(\frac{(\lambda_2 + \lambda_3)\Delta_1}{(\lambda_1 - \lambda_2)(\lambda_1 - \lambda_3)} p_1^2 + \frac{(\lambda_1 + \lambda_3)\Delta_2}{(\lambda_2 - \lambda_1)(\lambda_2 - \lambda_3)} p_2^2 + \frac{(\lambda_1 + \lambda_2)\Delta_3}{(\lambda_3 - \lambda_1)(\lambda_3 - \lambda_2)} p_3^2 \right),$$

$$F_2 = 2 \left(\frac{\lambda_2\lambda_3\Delta_1}{(\lambda_1 - \lambda_2)(\lambda_1 - \lambda_3)} p_1^2 + \frac{\lambda_1\lambda_3\Delta_2}{(\lambda_2 - \lambda_1)(\lambda_2 - \lambda_3)} p_2^2 + \frac{\lambda_1\lambda_2\Delta_3}{(\lambda_3 - \lambda_1)(\lambda_3 - \lambda_2)} p_3^2 \right),$$

where $\Delta_i = (a - \lambda_i)(b - \lambda_i)(c - \lambda_i)$.

Consider on the cotangent bundle of \mathbb{R}^3 three Poisson brackets $\{\cdot, \cdot\}_1$, $\{\cdot, \cdot\}_2$, $\{\cdot, \cdot\}_3$, defined by the following formulas.

$$\{f, g\}_i = \frac{\partial f}{\partial \lambda_i} \frac{\partial g}{\partial p_i} - \frac{\partial g}{\partial \lambda_i} \frac{\partial f}{\partial p_i} \quad \forall f, g \in C^\infty(T^*\mathbb{R}^3), \quad i = 1, 2, 3$$

We will call these Poisson brackets *partial*. Note that the sum of all partial brackets is the standard Poisson bracket on the cotangent bundle.

LEMMA 3.1. *The functions H, F_1, F_2 commute with respect to all partial Poisson brackets.*

PROOF. Let us prove this statement for functions H, F_1 and the first partial Poisson bracket. The other cases are analyzed analogously. Let us denote the functions $\frac{\Delta_i}{(\lambda_i - \lambda_j)(\lambda_i - \lambda_k)}$ by A_i , then

$$\begin{aligned} \{H, F_1\}_1 &= 8 \left(\frac{\partial A_1}{\partial \lambda_1} p_1^2 + \frac{\partial A_2}{\partial \lambda_1} p_2^2 + \frac{\partial A_3}{\partial \lambda_1} p_3^2 \right) (\lambda_2 + \lambda_3) A_1 p_1 \\ &- 8 \left((\lambda_2 + \lambda_3) \frac{\partial A_1}{\partial \lambda_1} p_1^2 + (\lambda_1 + \lambda_3) \frac{\partial A_2}{\partial \lambda_1} p_2^2 + (\lambda_1 + \lambda_2) \frac{\partial A_3}{\partial \lambda_1} p_3^2 + A_2 p_2^2 + A_3 p_3^2 \right) A_1 p_1 \\ &= 8 A_1 p_1 \left((\lambda_2 - \lambda_1) \frac{\partial A_2}{\partial \lambda_1} p_2^2 + (\lambda_3 - \lambda_1) \frac{\partial A_3}{\partial \lambda_1} p_3^2 + A_3 p_3^2 \right). \end{aligned}$$

It remains to take into account that the functions A_i satisfy the differential equations

$$(\lambda_i - \lambda_j) \frac{\partial A_i}{\partial \lambda_j} + A_i = 0 \quad \forall i \neq j.$$

The lemma is proved. \square

COROLLARY 3.1. *The functions H, F_1, F_2 commute with respect to the standard Poisson bracket.*

It turns out that the functions H, F_1, F_2 are functionally independent. This is established by the following lemma.

LEMMA 3.2. *The functions H, F_1, F_2 are functionally independent.*

PROOF. Let us consider the determinant of the Jacobi matrix of these functions on the momentum variables (we take the notation A_i from the proof of the previous lemma):

$$(3.2) \quad \frac{D(H, F_1, F_2)}{D(p_1, p_2, p_3)} = 64 p_1 p_2 p_3 A_1 A_2 A_3 \begin{vmatrix} 1 & 1 & 1 \\ \lambda_2 + \lambda_3 & \lambda_1 + \lambda_3 & \lambda_1 + \lambda_2 \\ \lambda_2 \lambda_3 & \lambda_1 \lambda_3 & \lambda_1 \lambda_2 \end{vmatrix}.$$

Note that the functions p_i, A_i do not vanish almost everywhere (they vanish on several hypersurfaces in $\mathbb{R}^6(\lambda_1, \lambda_2, \lambda_3, p_1, p_2, p_3)$). We show that the determinant on the right-hand side has a similar property, namely, it is zero if and only if $\lambda_i = \lambda_j$ for some $i \neq j$. For each column of the matrix on the right let us construct a polynomial with the same set of coefficients: $P_1(z) = z^2 + (\lambda_2 + \lambda_3)z + \lambda_2 \lambda_3 = (z + \lambda_2)(z + \lambda_3)$, $P_2(z) = z^2 + (\lambda_1 + \lambda_3)z + \lambda_1 \lambda_3 = (z + \lambda_1)(z + \lambda_3)$, $P_3(z) = z^2 + (\lambda_1 + \lambda_2)z + \lambda_1 \lambda_2 =$

$(z + \lambda_1)(z + \lambda_2)$. These polynomials are linearly dependent if and only if the determinant of the matrix in the formula 3.2 is zero.

Suppose that all λ_i are different, then none of P_i can be linearly expressed through the others, since $z = -\lambda_i$ is the root of all polynomials except P_i . If $\lambda_i = \lambda_j$ for some $i \neq j$, then the polynomials P_i and P_j coincide.

Hence, the set where the Jacobian 3.2 is not zero is open and everywhere dense in $T^*\mathbb{R}^3$, i.e., H, F_1, F_2 are functionally independent. The lemma is proved. \square

Note that the functions H, F_1, F_2 are conserved at reflection from the confocal quadric. Indeed, at reflection from the quadric, one of the impulses p_i changes sign to the opposite, while the others remain the same. And since the functions H, F_1, F_2 depend only on the squares of the impulses, they are conserved upon reflection from any confocal quadric. Thus, taking into account the lemmas 3.1, 3.2, billiards inside three-dimensional confocal regions are integrable by Liouville in a piecewise-smooth sense.

Now, we will show that the tangency polynomial always has 2 real roots, taking into account the multiplicity.

LEMMA 3.3. *At the common level h, f_1, f_2 of the first integrals H, F_1, F_2 , the equations of motion of the material point can be rewritten in the following form:*

$$(3.3) \quad \dot{\lambda}_i = \pm \frac{2\sqrt{2}}{(\lambda_i - \lambda_j)(\lambda_i - \lambda_k)} \sqrt{(a - \lambda_i)(b - \lambda_i)(c - \lambda_i)(h\lambda_i^2 - f_1\lambda_i + f_2)} \quad \forall i = 1, 2, 3.$$

PROOF. Note that $H\lambda_i^2 - F_1\lambda_i + F_2 = 2\Delta_i p_i^2$. Let us express p_i from this formula. Similarly, let us express $\dot{\lambda}_i$ from the equation $\dot{\lambda}_i = \partial H / \partial p_i$. By equating these expressions, we obtain the required formulas. The lemma is proved. \square

The following fact immediately follows from this lemma.

COROLLARY 3.2. *The tangency polynomial always has 2 real roots, taking into account the multiplicity, in other words, an arbitrary line in \mathbb{R}^3 is tangent to two confocal quadrics, taking into account the multiplicity.*

PROOF. Suppose that the tangent polynomial has no real roots. Then, according to the formula 3.3, the expression under the root must be negative on one of the intervals: (c, b) , (b, a) . However, this is, in general, impossible, since the motion on one of the elliptic coordinates would not be correctly defined. The corollary is proved. \square

This corollary is named after the famous French mathematician M. Chasles. Chasles's proof can be found in [29].

Thus, since the tangent polynomial always has two real roots, taking into account multiplicity, and the coefficients of this polynomial are the first integrals of the billiard, the roots of the tangent polynomial are also first integrals. And hence, all segments (or their extensions) of an arbitrary trajectory of a three-dimensional confocal billiard touch exactly two (taking multiplicity into account) common confocal quadrics. Thus, the theorem is completely proved. \square

It remains to answer one more important question. In what sense can some line touch a degenerate quadric? The answer to this question is given by the following proposition.

PROPOSITION 3.1.

1. The tangency of line l and the quadric of parameter $\lambda = c$ is equivalent to the fact that line l intersects the focal ellipse \mathfrak{F}_1 .
2. The tangency of the line l and the quadric of parameter $\lambda = b$ is equivalent to the fact that the line l intersects the focal hyperbola \mathfrak{F}_2 .
3. The tangency of the line l and the quadric of parameter $\lambda = a$ is equivalent to the fact that the line l lies in the plane $x = 0$.

PROOF. We restrict ourselves to the proof of the first point. The others are proved by analogy. The line l given in parametric form $(x + \tau\dot{x}, y + \tau\dot{y}, z + \tau\dot{z})$ passes through the focal ellipse \mathfrak{F}_1 if and only if the system

$$\begin{cases} z + \tau\dot{z} = 0, \\ \frac{(x + \tau\dot{x})^2}{a-c} + \frac{(y + \tau\dot{y})^2}{b-c} = 1, \end{cases}$$

has a solution (with respect to τ). Excluding τ from it, we obtain the equation (condition for system compatibility)

$$(b-c)(x\dot{z} - z\dot{x})^2 + (a-c)(y\dot{z} - z\dot{y})^2 = (a-c)(b-c)\dot{y}^2.$$

And this equation is exactly equivalent to the fact that $\lambda = c$ is the root of the tangent polynomial. To verify this, write the tangent polynomial in Cartesian coordinates and then substitute $\lambda = c$ into it. The proposition is proved. \square

The topology of the Liouville billiard foliation inside a three-axial ellipsoid was studied by V. Dragovich and M. Radnovich in [5]. They described the regular layers of this system and the structure of their 1-bifurcations. G. V. Belozero in his paper [24] described the regular layers and their 1-bifurcations for all three-dimensional confocal billiards.

4. Bifurcation diagrams. Singular layers

Starting from this section, we will study two kinds of three-dimensional confocal billiards: inside an ellipsoid (see Fig. 6.1), and in the region bounded by an ellipsoid and one sheet of a two-sheet hyperboloid (see Fig. 6.2).

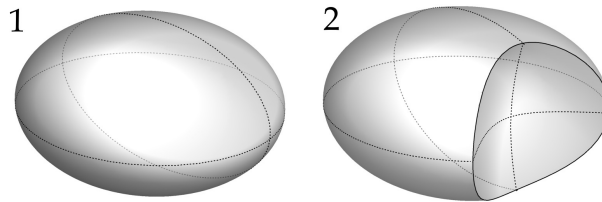


FIGURE 6. Non-separable billiard tables.

Why did we choose these tables? It turns out that only these regions contain parts of two focal curves. It is easy to observe this by looking at the classification of three-dimensional confocal billiard tables from the paper [24]. We will call such billiard tables *non-separable*. Throughout the following we will assume that the parameter of the ellipsoid included in the table boundary is equal to zero.

Separable tables are structured in some sense simpler. One of the elliptic coordinates on them is separated from the critical value. This property helps in describing the topology of the Liouville foliation of the corresponding billiard to lower the degree of freedom of the system. Therefore, the most difficult (from the point of view of describing the Liouville foliation) are billiards on non-separable tables.

According to the Theorem 3.1, all segments (or their extensions) of an arbitrary broken trajectory of a three-dimensional confocal billiard touch two common confocal quadrics (taking into account multiplicity). Let us denote the parameters of these quadrics by Λ_1 and Λ_2 . We will assume that $\Lambda_1 \geq \Lambda_2$. The replacement of (H, F_1, F_2) by $(H, \Lambda_1, \Lambda_2)$ is continuous and single-valued.

The functions H, Λ_1 and Λ_2 foliate M^6 into connected components of their common level surfaces. This partition generates the *Liouville foliation*. Our aim is to describe the semi-local structure of this foliation.

Consider the isoenergy surface $Q_h^5 = \{(x, v) \in M^6 | H = h\}$, where $h > 0$. Note that for different $h > 0$ the Liouville foliation on Q_h^5 is similarly arranged. This is indeed true, since the trajectory of the particle does not change as the energy changes. Only the time of motion along the trajectory changes. On an isoenergetic surface, consider the mapping $\mathcal{F} : Q_h^5 \mapsto \mathbb{R}^2$, that maps a point x from Q_h^5 to the values of the integrals $\Lambda_1(x)$ and $\Lambda_2(x)$. The mapping \mathcal{F} is the *momentum mapping*. Let us describe its image for the billiard tables under consideration.

1. Let \mathcal{Z}^3 be a region bounded by an ellipsoid. In this case, the coordinate λ_1 changes on the segment $[0, c]$, λ_2 changes on the segment $[c, b]$, λ_3 changes on the segment $[b, a]$. According to the formulae 3.3, the polynomial $V(z) = (a - z)(b - z)(c - z)(Hz^2 - F_1z + F_2)$ for almost all F_1, F_2 must take positive values on these intervals. Recall that by defn $Hz^2 - F_1z + F_2 = H(z - \Lambda_1)(z - \Lambda_2)$ and $\Lambda_1 \geq \Lambda_2$. If $\Lambda_1 < c$, then the polynomial $V(z)$ takes negative values on the interval (c, b) . Similarly, if $\Lambda_2 > b$, then $V(z) < 0$ on the interval (c, b) . So $\Lambda_1 \geq c$, $\Lambda_2 \leq b$. Thus, if $\Lambda_2 < 0$, then $V(z) < 0$ at $z \in (0, c)$. And if $\Lambda_1 > a$, then $V(z) < 0$ when $z \in (b, a)$. So $0 \leq \Lambda_1 \leq b$, $c \leq \Lambda_2 \leq a$, and $\Lambda_1 \geq \Lambda_2$. Exactly these three inequalities define the image of the mapping \mathcal{F} (see Fig. 7).

In the general case, the polynomial $V(z)$ has no multiple roots. The following 4 variants of the arrangement of the roots of $V(z)$ are possible (under the condition that there is no multiple root of $V(z)$):

1. $0 \leq \Lambda_1 < c < \Lambda_2 < b < a$;
2. $0 \leq \Lambda_1 < c < b < \Lambda_2 < a$;
3. $c < \Lambda_1 < \Lambda_2 < b < a$;
4. $c < \Lambda_1 < b < \Lambda_2 < a$.

The regions of possible motion (hereinafter referred to as RPMs) corresponding to each of these variants of the arrangement of the $V(z)$ roots are shown in Figure 8. Note that all these regions are different by their combinatorial structure.

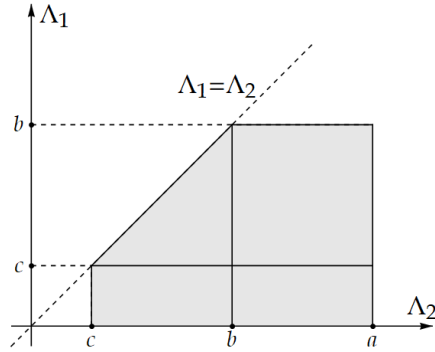


FIGURE 7. Momentum mapping $\mathcal{F}: Q_h^5 \mapsto \mathbb{R}^2(\Lambda_1, \Lambda_2)$ image (highlighted in grey). Black lines are bifurcation diagram

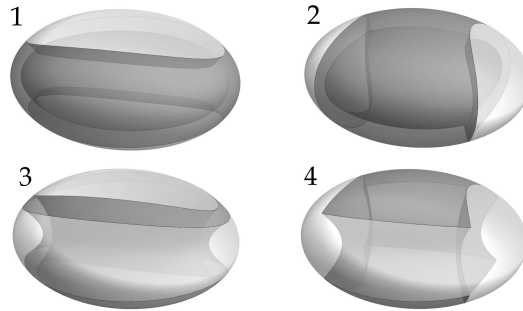


FIGURE 8. Types of regions of possible motion of a three-dimensional billiard inside an ellipsoid in the general case.

2. Now consider the table \mathcal{Z}^3 bounded by an ellipsoid of parameter 0 and a one-sheet hyperboloid of parameter $\lambda_0 > b$ (or by the plane $x = 0$). How will the image of the momentum mapping change in comparison to the Figure 7? If the table lies in one of the half-spaces $x \leq 0$ or $x \geq 0$, then in addition to the restrictions on Λ_i above, there is another one: $\Lambda_1 \leq \lambda_0$ (recall that the plane $x = 0$ is a quadric of parameter a). Otherwise, the image of the momentum mapping will be the same.

To describe typical regions of possible motion of such a billiard we need to intersect the table \mathcal{Z}^3 with typical regions of possible motion of the billiard inside the boundary ellipsoid. Again we obtain four types of RPMs.

Since the billiard system, in general, is not smooth, we are forced to introduce on our own the notion of regular and critical Liouville foliation layer. For this purpose, we note that the type of the region of possible motion changes when the polynomial $V(z)$ has a multiple root. We also note that on the boundary of the momentum mapping image, the system layers appear/disappear. Let us summarise these observations in the following definition.

DEFINITION 4.1. The point $L = (\Lambda_1, \Lambda_2)$ of the moment mapping image \mathcal{F} will be called *critical* if at least one of the following conditions is satisfied:

- The point L lies on the boundary of the moment mapping image.
- The polynomial $V(z) = H(a - z)(b - z)(c - z)(z - \Lambda_1)(z - \Lambda_2)$ has a multiple root.

The remaining points of the moment mapping image will be called *regular*. The layers corresponding to the critical (regular) points will be called *critical* (respectively *regular*).

DEFINITION 4.2. The set of the critical points of the moment mapping image \mathcal{F} will be called the *bifurcation diagram*.

The bifurcation diagram of a three-dimensional confocal billiard consists of several straight-line segments. The number of chambers of the diagram is four. Each camera corresponds to one type of RPM (see Fig. 8). We will number them by the numbers of the RPM types listed above. In Figure 7 the bifurcation diagram of the billiard inside an ellipsoid is shown.

DEFINITION 4.3. The *multiplicity* of the critical point $P = (\Lambda_1, \Lambda_2)$ will be the number of different straight-line segments of the bifurcation diagram that meet at L .

Note that the multiplicity of any point of the bifurcation diagram does not exceed 3.

For simplicity of explanation, we will divide all points of the bifurcation diagram into several classes.

DEFINITION 4.4. The point L of the bifurcation diagram will be called

- *right* if its multiplicity does not exceed two, otherwise *unright*;
- *boundary* if it lies on the boundary of the moment mapping image, otherwise *internal*;
- *angle* if it is right and is a vertex of a corner of the moment mapping image \mathcal{F} .

The unright critical points are exactly (c, c) and (b, b) .

In the next two sections, we give a description of the semi-local structure of Liouville foliation of two confocal billiards under consideration.

5. Liouville foliation near layers corresponding to right critical points

We divide this section into several parts, each of which is devoted to the study of the topology of Liouville foliation near layers corresponding to points of a certain kind. Some results given here (namely, theorems from the first and second paragraphs) were obtained by G. V. Beloszerov in [24] and are given without proof.

5.1. Regular layers. It turns out that a piecewise-smooth analogue of Liouville's theorem is true for all three-dimensional confocal billiards (not only for the two types that we consider).

THEOREM 5.1. *The inverse image of a regular point L under the moment mapping \mathcal{F} of an arbitrary three-dimensional confocal billiard is homeomorphic to a three-dimensional torus or an disjoint union of several three-dimensional tori. The Liouville foliation in a small neighbourhood of each such torus is trivial.*

The proof of this theorem can be found in [24]. Below we present Table 1, in which we list the number of Liouville tori corresponding to the chambers of bifurcation diagrams of the considering three-dimensional confocal billiards.

For convenience, we denote the region bounded by an ellipsoid by \mathcal{Z}_1 , and the region bounded by an ellipsoid and a sheet of a confocal two-sheet hyperboloid by \mathcal{Z}_2 . We will keep these notations throughout this and the following sections. We take the notation of the diagram cameras from the previous section.

TABLE 1. Number of three-dimensional tori corresponding to the chambers of the bifurcation diagrams.

\mathcal{Z}_1		\mathcal{Z}_2	
Chamber	Number of tori	Chamber	Number of tori
1	2	1	1
2	2	2	2
3	2	3	1
4	1	4	1

5.2. Layers corresponding to the right critical points of multiplicity 1.

Before we go to the description of the foliation near such layers, let us recall the notion of two-atoms introduced by A. T. Fomenko.

DEFINITION 5.1. Let $f = c$ be a critical value of a Morse function f on a compact orientable manifold M^2 . Let $\varepsilon > 0$ be chosen such that on the segment $[c - \varepsilon, c + \varepsilon]$ the point c is the unique critical value of f . The connected component of the set $f^{-1}([c - \varepsilon, c + \varepsilon])$ layered on the level lines of the function f is called the *2-atom*.

REMARK 5.1. All 2-atoms are considered with respect to a layer-by-layer diffeomorphism.

Let us give some examples of 2-atoms. According to Morse's lemma, in the neighbourhood of a nondegenerate singular point P , the function f is reduced to the form $f = f(P) \pm x^2 \pm y^2$. Therefore, if P is a point of minimum or maximum, the 2-atom corresponding to it is a disc layered by a family of concentric circles (see Fig. 9.1). Such an atom is called a *2-atom A*. There are infinitely many atoms corresponding to saddle singularities. In the present paper, we will need only two of them: B and C_2 . They are shown in Figures 9.2 and 9.3, respectively.

Note that the atom B is centrally symmetric. We denote the involution of the central symmetry of this atom by α . Hereafter we will use this notation. In

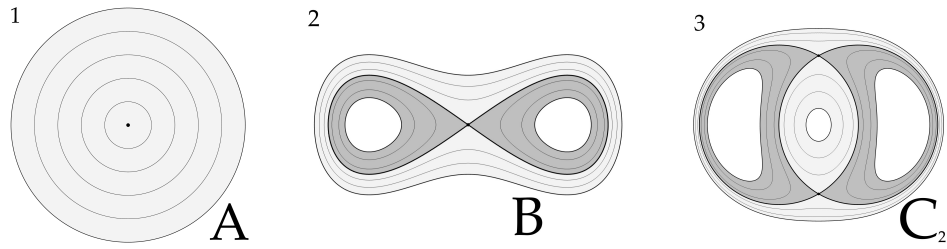


FIGURE 9. Examples of 2-atoms (from left to right): A , B , C_2 .

Figure 9, the atom C_2 is centrally symmetric, but it has more symmetries. Let us represent C_2 on a two-dimensional sphere as shown in Figure 10. Notice this figure has two rotational symmetries at angle π around the selected axes. We denote one of these symmetries by α and the other by β . To distinguish between them, we will call one of them - *the first rotational symmetry* and the other - *the second rotational symmetry*.

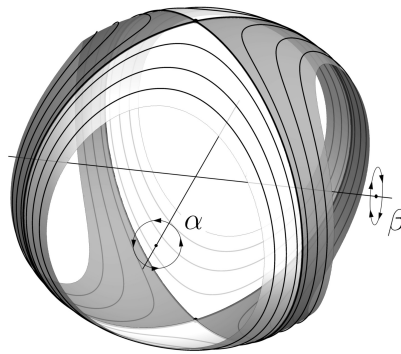


FIGURE 10. Rotational symmetries of the atom C_2 on the two-dimensional sphere.

According to the results of N. T. Zung, Liouville foliation in the neighbourhood of many saddle nondegenerate singularities is representable as an almost direct product of 2-atoms (see, e.g., [37]).

Bifurcations of systems with two degrees of freedom on surfaces of constant energy are described by means of 3-atoms introduced by Fomenko. The reader can find more details about 3-atoms in [38]. Hereafter we use only 2-atoms. Nevertheless, we recall that the almost direct product $(B \times S^1)/\mathbb{Z}_2(\alpha)$, where α is the involution acting by the central symmetry on the terms, is the 3-atom A^* .

Let us return to three-dimensional billiards. The following theorem holds.

THEOREM 5.2. *Let L be a critical point of multiplicity 1 of the three-dimensional billiard on \mathcal{Z}_1 or \mathcal{Z}_2 , then*

- if L is an interior point, then the small neighbourhood of the layer corresponding to it is layer-by-layer homeomorphic to a direct product of the form $V^{(3)} \times S^1 \times \bar{D}^1$, where \bar{D}^1 is a segment, and $V^{(3)}$ is one of the following 3-atoms: $(B \times S^1)/\mathbb{Z}_2(\alpha)$ (here α is the involution of central symmetry), $B \times S^1$, $C_2 \times S^1$.
- if L is a boundary point, then the small neighbourhood of the layer corresponding to it is layer-by-layer homeomorphic to a direct product of the form $A \times S^1 \times S^1 \times \bar{D}^1$.

The proof of this fact for an arbitrary confocal billiard table is given in [24].

5.3. Layers corresponding to right critical points of multiplicity 2.

The layers corresponding to the point (b, c) (we will call it the cross point) are the most difficult to study. Therefore, we will start from this point.

THEOREM 5.3.

1. The small neighbourhood (in Q_h^5) of the Liouville foliation layer corresponding to the point (b, c) , of the billiard inside a three-axial ellipsoid, i.e. on \mathcal{Z}_1 , is layer-by-layer homeomorphic to the almost direct product $\frac{B \times C_2}{\mathbb{Z}_2(\alpha)} \times S^1$, where the involution α acts by central symmetry on B and rotational symmetry on C_2 .
2. The small neighbourhood (in Q_h^5) of the Liouville foliation layer, corresponding to the point (b, c) , of the billiard inside \mathcal{Z}_2 is layer-by-layer homeomorphic to the almost direct product $\frac{B \times C_2 \times S^1}{\mathbb{Z}_2(\alpha) \times \mathbb{Z}_2(\beta)}$, where the involution α acts by the central symmetry on the atom B and by the first rotational symmetry on the atom C_2 (on S^1 acts trivially), and the involution β acts by the second rotational symmetry on the atom C_2 and by the central symmetry on the circle S^1 (on B acts trivially).

PROOF. Let us prove the first point of the theorem. Consider a billiard inside the ellipsoid of parameter 0, i.e. on the table \mathcal{Z}_1 . Let $L = (b, c)$. Let us denote by T_L the inverse image of the point L under the momentum mapping \mathcal{F} . The point L corresponds to the critical circle $\gamma(L)$ arising at the motion of the particle along the axis Ox .

It turns out that on Liouville tori $T_{L'}$ close to T_L one can choose a cycle $\gamma(L')$ homologous to $\gamma(L)$, which will transform into $\gamma(L)$ when L' tends to L . This is clearly shown in Figure 11 for all four kinds of Liouville tori corresponding to the chambers of the bifurcation diagram.

The billiard system inside an ellipsoid is smoothenable, and the forms $\alpha = p_1 d\lambda_1 + p_2 d\lambda_2 + p_3 d\lambda_3$ and $\omega = dp_1 \wedge d\lambda_1 + dp_2 \wedge d\lambda_2 + dp_3 \wedge d\lambda_3$ are correctly defined on the phase space of the system. This follows from the results of V. Lazutkin [40] and E. A. Kudryavtseva [41]. Let us consider in a small neighbourhood of T_L on the regular parts of the Liouville foliation the function

$$s(L') = \frac{1}{2\pi} \int_{\gamma(L')} \alpha.$$

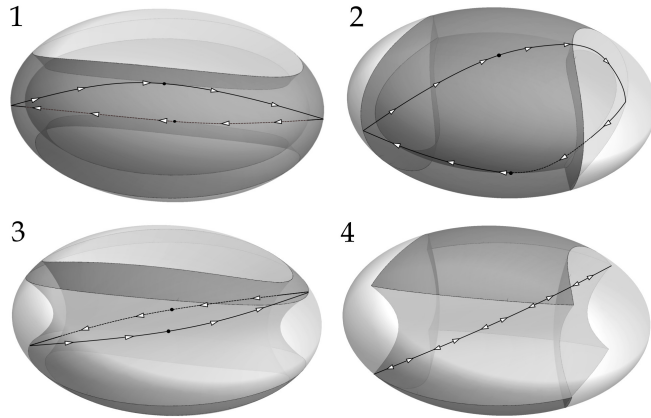


FIGURE 11. A cycle γ on Liouville tori close to the isointegral surface $\mathcal{F}^{-1}(b, c)$ in Q_h^5 . The highlighted points are the tangency points of the cycle with the inner ellipsoid (Figures 1, 2) and the inner one-sheet hyperboloid (Figure 3).

Let us find the explicit form of the function $s(L')$. According to the formulae of separation of variables 3.2, the following equations hold

$$p_i^2 = \frac{h}{2} \frac{(\lambda_i - \Lambda_1)(\lambda_i - \Lambda_2)}{(a - \lambda_i)(b - \lambda_i)(c - \lambda_i)} \quad \forall i = 1, 2, 3.$$

The γ cycle traverses each elliptic coordinate exactly twice (from maximum to minimum value and back again). Hence,

$$s(H, \Lambda_1, \Lambda_2) = \frac{1}{\pi} \int_0^{\Lambda_2 \wedge c} \sqrt{2h \frac{(t - \Lambda_1)(t - \Lambda_2)}{(a - t)(b - t)(c - t)}} dt + \frac{1}{\pi} \int_{c \vee \Lambda_2}^{\Lambda_1 \wedge b} \sqrt{2h \frac{(t - \Lambda_1)(t - \Lambda_2)}{(a - t)(b - t)(c - t)}} dt + \frac{1}{\pi} \int_{\Lambda_1 \vee b}^a \sqrt{2h \frac{(t - \Lambda_1)(t - \Lambda_2)}{(a - t)(b - t)(c - t)}} dt.$$

In the latter formula, the expression $P \wedge Q$ means the minimum between P and Q , and $P \vee Q$ means the maximum between them.

LEMMA 5.1. *The function $s(H, \Lambda_1, \Lambda_2)$ is analytic in a small neighbourhood of the point L .*

PROOF. Let $\Lambda_1 \neq b, \Lambda_2 \neq c$. Consider on the complex plane the contour C shown in Figure 12. It consists of the arc Γ of the upper semicircle connecting the points 0 and a , four semicircles Γ_ε of radii ε with centres at points $c, b, \Lambda_1, \Lambda_2$ and five segments. Let us choose the positive direction on the contour. Let

$$f(z) = \frac{1}{\pi} \sqrt{2h \frac{(z - \Lambda_1)(z - \Lambda_2)}{(a - z)(b - z)(c - z)}}.$$

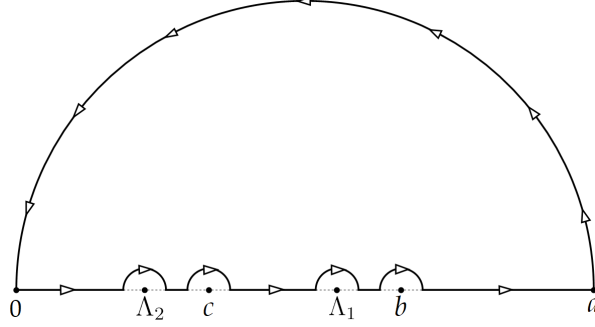


FIGURE 12. Integration contour.

According to Cauchy's integral theorem

$$0 = \oint_{C^+} f(z)dz = \int_{\Gamma^+} f(z)dz + I_1(\varepsilon) + I_2(\varepsilon) + I_3(\varepsilon),$$

where

$$\begin{aligned} I_1(\varepsilon) &= \int_0^{\Lambda_2 - \varepsilon \wedge c - \varepsilon} f(z)dz + \int_{c + \varepsilon \vee \Lambda_2 + \varepsilon}^{\Lambda_1 - \varepsilon \wedge b - \varepsilon} f(z)dz + \int_{b + \varepsilon \vee \Lambda_1 + \varepsilon}^a f(z)dz, \\ I_2(\varepsilon) &= \int_{\Lambda_2 + \varepsilon \wedge c + \varepsilon}^{\Lambda_2 - \varepsilon \vee c - \varepsilon} f(z)dz + \int_{b + \varepsilon \wedge \Lambda_1 + \varepsilon}^{\Lambda_1 - \varepsilon \vee b - \varepsilon} f(z)dz \\ I_3(\varepsilon) &= \int_{\Gamma_\varepsilon^-(\Lambda_1)} f(z)dz + \int_{\Gamma_\varepsilon^-(\Lambda_2)} f(z)dz + \int_{\Gamma_\varepsilon^-(c)} f(z)dz + \int_{\Gamma_\varepsilon^-(b)} f(z)dz. \end{aligned}$$

Note that $s = \lim_{\varepsilon \rightarrow 0} I_1(\varepsilon)$, and $I_2(\varepsilon)$ is a pure imaginary number. At the same time, $\lim_{\varepsilon \rightarrow 0} I_3(\varepsilon) = 0$. Indeed, this fact follows from the standard inequality:

$$\left| \oint_{\gamma} f(z)dz \right| \leq \max_{z \in \gamma} |f(z)| \cdot |\gamma|.$$

So,

$$(5.1) \quad s = \frac{1}{\pi} \operatorname{Re} \int_{\Gamma^-} \sqrt{2h \frac{(z - \Lambda_1)(z - \Lambda_2)}{(a - z)(b - z)(c - z)}} dz.$$

Since there are no points $c, b, \Lambda_1, \Lambda_2$ on the contour Γ , the function s is correctly defined and analytic in a small neighbourhood of the point $L = (b, c)$. Lemma 4 is proved. \square

The function s is an action variable. Moreover, according to the formula 5.1 it is smooth in a small neighbourhood of the layer T_L in M^6 . Let us denote by $U(L)$ a small enough closed neighbourhood of the layer T_L in Q_h^5 .

LEMMA 5.2. *Vector field $v = \operatorname{sgrad} s$*

1. *is not zero in $U(L)$;*
2. *is transversal to the submanifold $\hat{M}^4 = \{(x, v) \in U(L) | x = 0\}$.*

PROOF. We restrict ourselves to the proof of the second point. The proof of the first part requires a detailed analysis of the ranks of the system dH, dF_1, dF_2 on smooth parts of the phase space, which we will not describe here.

Using the chain rule, as well as the explicit form of the first integrals H, F_1, F_2 , in the regions of nondegeneracy of elliptic coordinates, we obtain the following equalities:

$$\begin{aligned} \frac{\partial s}{\partial p_i} &= \frac{\partial s}{\partial H} \frac{\partial H}{\partial p_i} + \frac{\partial s}{\partial F_1} \frac{\partial F_1}{\partial p_i} + \frac{\partial s}{\partial F_2} \frac{\partial F_2}{\partial p_i} \\ &= \frac{1}{\pi\sqrt{2H}} \frac{\partial H}{\partial p_i} \operatorname{Re} \int_{\Gamma^-} \frac{(z - \lambda_j)(z - \lambda_k)}{\sqrt{(a-z)(b-z)(c-z)(z - \Lambda_1)(z - \Lambda_2)}} dz \end{aligned}$$

At the common level of the first integrals Λ_1 and Λ_2 in Q_h^5 , the vector field v defines the following system of first order differential equations:

$$(5.2) \quad \dot{\lambda}_i = \pm \frac{2\sqrt{\Delta(\lambda_i)(\lambda_i - \Lambda_1)(\lambda_i - \Lambda_2)}}{\pi(\lambda_i - \lambda_j)(\lambda_i - \lambda_k)} \operatorname{Re} \int_{\Gamma^-} \frac{(z - \lambda_j)(z - \lambda_k)}{\sqrt{\Delta(z)(z - \Lambda_1)(z - \Lambda_2)}} dz$$

Here $\Delta(z) = (a-z)(b-z)(c-z)$.

Recall that the mapping $\pi : M^6 \mapsto \mathcal{Z}_1$, which maps a point-vector pair (x, v) to a point x , is correctly defined. Let us compute the value \dot{x} of the projection π_* of the vector field v on the billiard table. The pairs $(x, v) \in \hat{M}^4$ satisfy the condition $x = 0$, i.e., $\lambda_3 = a$. Since $\lambda = a$ is a degenerate quadric, we cannot compute \dot{x} using the chain rule. However, we will use it by applying the limit transition

$$\dot{x} = \lim_{\lambda_3 \rightarrow a} \left(\frac{\partial x}{\partial \lambda_1} \dot{\lambda}_1 + \frac{\partial x}{\partial \lambda_2} \dot{\lambda}_2 + \frac{\partial x}{\partial \lambda_3} \dot{\lambda}_3 \right).$$

According to the formulae 5.2, the derivatives $\dot{\lambda}_1, \dot{\lambda}_2$ tend to zero at $\lambda_3 \rightarrow a$. Thus, $\frac{\partial x}{\partial \lambda_1}, \frac{\partial x}{\partial \lambda_2}$ are bounded functions at $\lambda_3 = a$. Hence,

$$(5.3) \quad \dot{x} = \lim_{\lambda_3 \rightarrow a} \frac{\partial x}{\partial \lambda_3} \dot{\lambda}_3.$$

To prove the second point of the lemma, we only need to show that \dot{x} is different from zero for $\Lambda_1 = b, \Lambda_2 = c$. Using the formulae 3.1, 5.2, and the limit relation 5.3, we conclude that

$$\dot{x} = \pm \frac{1}{\pi} \sqrt{\frac{(a-b)(a-c)}{(a-\lambda_1)(a-\lambda_2)}} \operatorname{Re} \int_{\Gamma^-} \frac{(z - \lambda_1)(z - \lambda_2)}{\sqrt{a-z(b-z)(c-z)}} dz.$$

It remains to prove that the integral in the last formula is nonzero. Using the methods of integration of functions of complex variable (see lemma 5.1), it is easy to show that

$$\operatorname{Re} \int_{\Gamma^-} \frac{(z - \lambda_1)(z - \lambda_2)}{\sqrt{a-z(b-z)(c-z)}} dz = \text{v.p.} \int_0^a \frac{(t - \lambda_1)(t - \lambda_2)}{\sqrt{a-t(b-t)(c-t)}} dt.$$

The integral on the right-hand side can be calculated explicitly. Indeed, let us simplify the part of the expression under the integral.

$$\frac{(t - \lambda_1)(t - \lambda_2)}{(b - t)(c - t)} = 1 + \frac{(b - \lambda_1)(b - \lambda_2)}{(b - c)(t - b)} + \frac{(c - \lambda_1)(c - \lambda_2)}{(c - b)(t - c)}$$

For a more compact notation, we denote the coefficients before $\frac{1}{t-b}$ and $\frac{1}{t-c}$ by C_1 and C_2 . Note that both of these numbers are positive. Thus,

$$\begin{aligned} & \text{v.p.} \int_0^a \frac{(t - \lambda_1)(t - \lambda_2)}{\sqrt{a-t}(b-t)(c-t)} dt \\ &= \int_0^a \frac{dt}{\sqrt{(a-t)}} + C_1 \text{v.p.} \int_0^a \frac{dt}{\sqrt{a-t}(t-b)} + C_2 \text{v.p.} \int_0^a \frac{dt}{\sqrt{a-t}(t-c)} \\ &= 2\sqrt{a} + \frac{C_1}{\sqrt{a-b}} \ln \frac{\sqrt{a} + \sqrt{a-b}}{\sqrt{a} - \sqrt{a-b}} + \frac{C_2}{\sqrt{a-c}} \ln \frac{\sqrt{a} + \sqrt{a-c}}{\sqrt{a} - \sqrt{a-c}}. \end{aligned}$$

In the last sum, all terms are greater than zero. So $\dot{x} \neq 0$ on \hat{M}^4 . Thus, lemma 5 is proved. \square

It follows from the second point of lemma 5.2 that the manifold \hat{M}^4 consists of two layer-by-layer homeomorphic connectivity components. We denote by \hat{M}_+ the component satisfying the restriction $\dot{x} > 0$ (the other component is denoted by \hat{M}_-).

According to the classical theory of integrable systems, the trajectories of the field v are closed and its integral curves are 2π -periodic. Moreover, the trajectories of v , on the layer $T_{L'}$ (close to T_L), are homologous to cycles $\gamma(L')$, which are homologous to $\gamma(L)$ by their definition. Now, using the vector field v , we show that the neighbourhood $U(L)$ has a trivial S^1 -fibration.

Consider the Cauchy problem of a vector field v with initial points on a submanifold \hat{M}_+ . We obtain a flow g_t under the action of which the manifold \hat{M}_+ “deforms” in Q_h^5 . However, note that $g_{2\pi} = g_0 = \text{id}$. In other words, in time $t = 2\pi$ the manifold \hat{M}_+ returns to its initial position. Thus, we obtain the mapping $G : \hat{M}_+ \times S^1 \rightarrow U(L)$ given by the formula $G(x, t) = g_t(x)$. The following lemma establishes a key property of the mapping G .

LEMMA 5.3. *The mapping G is a homeomorphism between $\hat{M}_+ \times S^1$ and $U(L)$.*

PROOF. The mapping G is continuous. This fact follows from the theorem on the continuous dependence of the solution of the Cauchy problem on the initial data.

Now we show that G is bijective. The manifold \hat{M}_+ intersects every Liouville torus $T_{L'}$ close to the layer T_L by a two-dimensional torus $\hat{T}_{L'}$. Note that the trajectories of the field $v = \text{sgrad } s$ are basis cycles complementing any basis on the 2-torus $\hat{T}_{L'}$ to the basis on the 3-torus $T_{L'}$. This is not difficult to verify. Indeed, let μ_i be basis cycles on the torus T_L corresponding to the motion along the i -Theorem elliptic coordinate. Then (μ_1, μ_2, μ_3) is a basis on T_L , and (μ_1, μ_2) is a basis on $\hat{T}_{L'}$. The trajectories v are homologous to $\nu = k_1\mu_1 + k_2\mu_2 + \mu_3$ for some integers k_1 and k_2 . Hence, the triple (μ_1, μ_2, ν) is a basis on $T_{L'}$.

The trajectories of the system v drawn from different points $\hat{T}_{L'}$ cannot intersect. Indeed, let us choose angular variables $(\varphi_1, \varphi_2, \varphi_\nu)$ on the Liouville torus corresponding to the cycles μ_1, μ_2 and ν , respectively. The vector field v will then coincide with $\frac{\partial}{\partial \varphi_\nu}$. Since the coordinate lines φ_1 and φ_2 are homologous to the cycles μ_1 and μ_2 , which in turn are basic on the torus $\hat{T}_{L'}$, this two-dimensional torus can be represented in $\mathbb{R}^3(\varphi_1, \varphi_2, \varphi_\nu)$ as a membrane stretched on the lateral boundary of a cylinder with a base as a square $(\varphi_1, \varphi_2) \in [0, 2\pi]^2$. And since the field v is transversal to \hat{M} at each point, the surface \hat{M} is locally defined as the graph of the function $\varphi_\nu = f(\varphi_1, \varphi_2)$. Based on the last two facts, we conclude that the torus $\hat{T}_{L'}$ is the graph of the 2π -periodic function at coordinates φ_1, φ_2 in $\mathbb{R}^3(\varphi_1, \varphi_2, \varphi_\nu)$. Since any line parallel to the axis $O\varphi_\nu$ intersects this graph at a single point, the trajectories of the field v drawn from different points of $\hat{T}_{L'}$ cannot intersect. Hence, we obtain the injectivity and surjectivity of G on every Liouville torus. Hence, the image of the mapping G is everywhere dense in $U(L)$. Since $\hat{M}_+ \times S^1$ is compact and the continuous compact image is compact, the mapping image G is closed. So, the image of the mapping G is the neighbourhood $U(L)$. Thus, the surjectivity of G is proved.

Let us show the injectivity. For small values of the parameter t the injectivity of G is obvious (the vector field v is transversal to \hat{M}_+). Let us choose ε such that the restriction G on $Q' = \hat{M}_+ \times [-\varepsilon, \varepsilon]$ is injective. Then due to the compactness of Q' , the mapping G establishes a homeomorphism between Q' and $G(Q')$. Thus, $\text{Int } Q'$ and Q^5 are topological manifolds. Hence, for any point $(x, 0) \in Q'$ there is a small neighbourhood of U such that $G(U)$ is open in Q^5 .

Suppose now that $G(x_1, t_1) = G(x_2, t_2)$. Due to the group property of the flow g_t we have $G(x_1, 0) = G(x_2, t_2 - t_1)$. Let us choose non-intersecting neighbourhoods U and V of points $(x_1, 0)$ and $(x_2, t_2 - t_1)$ such that $G(U)$ is open in Q^5 . Then the set $V \cap G^{-1}(G(U))$ is a neighbourhood of the point $(x_2, t_2 - t_1)$. Thus, V contains an open everywhere dense subset consisting of pairs (x, t) where x lies on tori $\hat{T}_{L'}$. However, this subset must be injectively mapped to $G(U)$ due to the injectivity of G on Liouville tori, but the restriction of G to U is a homeomorphism. Therefore, U and V must intersect. Contradiction. Thus, G is injective.

Since \hat{M}_+ and S^1 are compact and the mapping G is a continuous bijection, G is a homeomorphism. Thus, lemma 6 is proved. \square

Let us restrict the Liouville foliation from Q^5 to \hat{M}_+ . By multiplying each layer by a circle, we obtain a foliation on the manifold $\hat{M}_+ \times S^1$. In fact, the lemma 5.3 claims more: $U(L)$ and $\hat{M}_+ \times S^1$ are layer-by-layer homeomorphic. Therefore, to complete the proof of the first point, it remains to describe the Liouville foliation on \hat{M}_+ .

Let us consider the equations of motion 3.2 induced on \hat{M}_+ . Since the third elliptic coordinate is fixed on \hat{M}_+ and $\dot{x} > 0$, let us look at the equations of the first two coordinates. We obtain

$$\dot{\lambda}_1 = \pm \frac{2\sqrt{2}}{(\lambda_2 - \lambda_1)(a - \lambda_1)} \sqrt{h(\lambda_1 - \Lambda_1)(\lambda_1 - \Lambda_2)(a - \lambda_1)(b - \lambda_1)(c - \lambda_1)},$$

$$\dot{\lambda}_2 = \pm \frac{2\sqrt{2}}{(\lambda_1 - \lambda_2)(a - \lambda_2)} \sqrt{h(\lambda_2 - \Lambda_1)(\lambda_1 - \Lambda_2)(a - \lambda_2)(b - \lambda_2)(c - \lambda_2)},$$

Since $\lambda_1, \lambda_2 < a$, avoiding multipliers of the form $a - \lambda_i$ will not change the topology of the Liouville foliation on \hat{M}_+ . The resulting system of equations

$$\begin{aligned} \dot{\lambda}_1 &= \pm \frac{2\sqrt{2}}{\lambda_2 - \lambda_1} \sqrt{h(\lambda_1 - \Lambda_1)(\lambda_1 - \Lambda_2)(b - \lambda_1)(c - \lambda_1)}, \\ \dot{\lambda}_2 &= \pm \frac{2\sqrt{2}}{\lambda_1 - \lambda_2} \sqrt{h(\lambda_1 - \Lambda_1)(\lambda_2 - \Lambda_2)(b - \lambda_2)(c - \lambda_2)}, \end{aligned}$$

defines the dynamics of a material point on the plane in a field of elastic force of a coefficient $k < 0$. Since the plane $x = 0$ intersects the table \mathcal{Z}_1 on the region bounded by an ellipse with semi-axes b and c , we conclude that \hat{M}_+ is layer-by-layer homeomorphic to the small neighbourhood of the singular layer of a rank 0 point of the billiard in a Hooke potential field inside this ellipse. According to the results of V. A. Kibkalo and A. T. Fomenko (see [43]), this neighbourhood is homeomorphic to the almost direct product of 2-atoms B and C_2 factorised by the involution α acting by the central symmetry on atom B and by the rotational symmetry on C_2 . Thus, $U(L)$ is layer-by-layer homeomorphic to $(B \times C_2)/\mathbb{Z}_2(\alpha) \times S^1$.

Let's proceed to the second item. Consider a table \mathcal{Z}_2 bounded by an ellipsoid of parameter 0 and the plane $x = 0$. We will assume that it is located in the half-space $x \geq 0$. In the other cases, the proof will be similar. In order to describe the topology of Liouville foliation in a small neighbourhood $U(L)$ of the layer corresponding to the point $L = (b, c)$, we return to the action variable construction from the first item.

Note that g_π transforms \hat{M}_+ into \hat{M}_- . Due to the symmetry of the ellipsoid with respect to the coordinate planes, a point from \hat{M} with Cartesian coordinates $(0, y, z)$ and velocity vector v move to a point with coordinates $(0, -y, -z)$ and velocity vector $-v$ in time $t = \pi$.

If we consider a billiard inside the table \mathcal{Z}_2 , a reflection must occur on the wall $x = 0$. During the time $t \in [0, \pi)$ the surfaces $g_t(\hat{M}_+)$ will go round the whole neighbourhood $U(L)$, and at $t = \pi$ the set \hat{M}_+ will return to the initial position but with "spin". Let us describe how it is organised.

The almost direct product $(B \times C_2)/\mathbb{Z}_2(\alpha)$ from the first item of the theorem has a natural central symmetry. Indeed, according to the paper [43] this product is realised as a small neighbourhood of a saddle-saddle layer of billiard in a Hooke's repulsive potential field inside an ellipse. However, in such a system there is the natural symmetry τ mapping the point-vector pair (P, v) into the pair $(-P, -v)$.

Due to the structure of the mapping g_π and the reflection from the wall $x = 0$, we conclude that the neighbourhood $U(L)$ is layer-by-layer homeomorphic to the almost direct product of the circle S^1 and the product $(B \times C_2)/\mathbb{Z}_2(\alpha)$, factorised by the involution τ acting on S^1 and $(B \times C_2)/\mathbb{Z}_2(\alpha)$ by the central symmetry. Let us simplify this product.

The symmetry τ is realised due to the additional rotational symmetry β on the atom C_2 . Therefore, the neighbourhood $U(L)$ is layer-by-layer homeomorphic

to $(B \times C_2 \times S^1) / \mathbb{Z}_2(\alpha) \times \mathbb{Z}_2(\beta)$, where α acts by the central symmetry on B and by the first rotational symmetry on C_2 (on the circle the action is trivial), and β acts by the second rotational symmetry on C_2 and by the central symmetry on the circle (on B the action is trivial). Thus, the theorem is completely proved. \square

We give the following theorem without proof. It describes the structure of Liouville foliation near the layers corresponding to the boundary points of multiplicity 2.

THEOREM 5.4. *Let L be a boundary critical point of multiplicity 2 of the billiard on table \mathcal{Z}_1 or \mathcal{Z}_2 , then the inverse image of a small neighbourhood of L (in Q_h^5) under the momentum mapping \mathcal{F} is layer-by-layer homeomorphic to a disjoint union of several direct products of the form*

- $A \times B \times S^1$, $A \times C_2 \times S^1$, $A \times (B \times S^1) / \mathbb{Z}_2(\alpha)$ if L is a non-angle point. Here α is the involution of central symmetry;
- $A \times A \times S^1$ if L is an angle point.

The idea of the proof of the theorem 5.4 is based on the method of lowering the degrees of freedom of the system, which we used in the proof of the theorem 5.3. We need to change the shape of the table so that the table does not contain parts of one of the focal curves. This transformation will not change the topology of the Liouville foliation. Indeed, since the pair (Λ_1, Λ_2) belongs to the boundary of the momentum mapping image, with a small change of Λ_i the particle will not reach the focal curves. As a result of this transformation, the table will decompose into a direct product of tables of lower dimension. And the singularity will decompose into a direct product of singularities of integrable billiards on these tables.

6. Liouville foliation near layers corresponding to unright critical points

Let us recall the definition of two important degenerate singularities which arise quite often in integrable systems of two degrees of freedom. For this purpose, consider two functions $H = z$ and $F = x^2 + y^4 - zy^2$ in the space $\mathbb{R}^3(x, y, z) \times S^1(\varphi)$. The set of critical points of the system of these two functions at a fixed value of φ is a ‘‘pitchfork’’, i.e. the union of a parabola and its axis (see Fig. 13).

The functions H and F define a foliation $\mathbb{R}^3(x, y, z) \times S^1(\varphi)$ on the connected components of their common level (analogue of Liouville foliation). In the neighborhood of critical points, this foliation looks as shown in Figure 13. Let $X > 0$. Consider the part of the foliation in the neighborhood of the set of critical points that falls in the zone $|z| \leq X$. This neighborhood, layered on the level lines of functions H and F , is called the *orientable elliptic pitchfork*. We note that the group \mathbb{Z}_2 of rotation symmetry on π around the axis Oz acts on the orientable elliptic pitchfork. The factor on this action is called *non-orientable elliptic pitchfork*.

Such degenerate singularities (and many others) appeared in [42] while investigating the Liouville foliation topology of the Kovalevskaya top.

We will denote the orientable elliptic pitchfork by PF_o and the non-orientable pitchfork by PF_{no} .

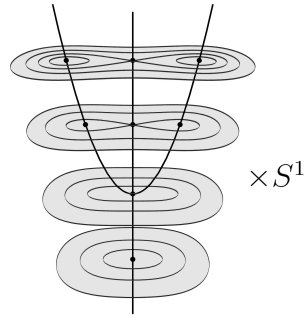


FIGURE 13. Elliptic pitchfork.

THEOREM 6.1. *Let L be an unright critical point. Table 2 defines the structure of Liouville foliation of billiard on table \mathcal{Z}_1 or \mathcal{Z}_2 in a small neighborhood of the layer corresponding to the point L .*

TABLE 2. Liouville foliation near layers corresponding to unright critical points.

\mathcal{Z}_1		\mathcal{Z}_2	
Point	Foliation	Point	Foliation
(b, b)	$PF_o \times S^1$	(b, b)	$PF_{no} \times S^1$
(c, c)	$2PF_{no} \times S^1$	(c, c)	$PF_{no} \times S^1$

PROOF. We consider a table bounded by an ellipsoid, i.e., \mathcal{Z}_1 , and describe the Liouville foliation in the neighborhood of the layer T_P corresponding to the point $L = (b, b)$. The proof for the point (c, c) as well as for the table \mathcal{Z}_2 is carried out by analogy.

Let the point L' be close to L , then the region of possible motion corresponding to this point is separated by the second elliptic coordinate from the value c . So, such a region can be trivially layered by confocal ellipsoids (and by the Oxy plane). In this case, the Liouville foliation will be the same on each such layer. Moreover, applying the reasoning from the proof of Theorem 5.3, we conclude that the neighborhood $U(L)$ in Q_h^5 of layer L is layer-by-layer homeomorphic to the direct product of the circle and $\hat{M}_+^4 \cap U(L)$ (recall that $\hat{M}_+^4 = \{(x, v) \in Q_h^5 | x = 0, \dot{x} > 0\}$). Based on the reasoning above, we conclude that $U(L)$ is layer-by-layer homeomorphic to the direct product of the two-dimensional torus and the complex K^3 , where K^3 is a 3-complex, obtained by restricting the neighborhood $U(L)$ to an ellipse lying in the plane $x = 0$ and given by the equation $\frac{y^2}{b} + \frac{z^2}{c} = 1$, taken together with the tangent vectors such that $\dot{x} > 0$. Let us describe how the Liouville foliation on K^3 is organized.

Let us foliate a small neighborhood of the point L by a one-parameter family of arcs $l(t)$, $t \in [0, 1]$, as shown in Figure 14.1.

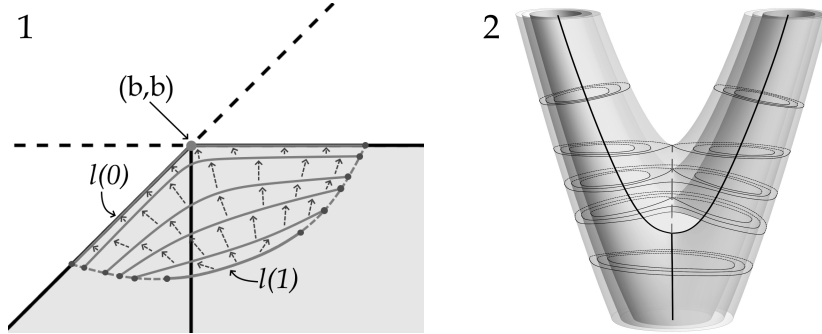


FIGURE 14. 1. The foliation of a small neighborhood of the point (b, b) of the bifurcation diagram by a one-parameter family of arcs $l(t)$, $0 \leq t \leq 1$. 2. Homotopy of the 2-atom B into its base. The line of critical points of B -atoms is dotted.

The K^3 restriction on $l(t)$ at $t > 0$ is homeomorphic to the 2-atom B . At $t = 0$ this restriction is homeomorphic to the letter Y . Hence, the complex K^3 represents the deformation of the 2-atom B into its base (see Fig. 14.2). If we select the line of critical points of B atoms corresponding to the arcs $l(t)$, $t > 0$, we obtain the complex shown on the left in Figure 14. Thus, the small neighborhood of layer T_L is layer-by-layer homeomorphic to the direct product of an orientable elliptic pitchfork and a circle. The theorem is proved. \square

7. Action variables and their use in proving Staudé's construction

Staudé's method of constructing a tree-axial ellipsoid using a thread was described in the second section. Below we give a proof of this method using action variables.

First, consider the billiard inside the ellipse $\frac{x^2}{a} + \frac{y^2}{b} = 1$. Its first integral is the parameter Λ of the quadric confocal with the ellipse, which is touched by all segments of the broken trajectory (or their extensions). The saddle critical value of this integral on the isoenergetic surface Q_h^3 is $\Lambda = b$. It turns out that in the neighborhood of the corresponding critical layer in Q_h^3 one of the action variables can be smoothly extended. For this purpose, on the layers close to the critical layer, we must choose a cycle γ that "passes" each elliptic coordinate exactly twice (i.e., runs twice from the minimum value of the coordinate on the layer to the maximum value and back again). These cycles, on layers close to $\Lambda = b$, are shown in Figures 15.1-2. Integrating the form $\alpha = v_1 dx + v_2 dy$ over these cycles (here v_1, v_2 are the coordinates of the velocity vector in the $\partial/\partial x, \partial/\partial y$ basis) and dividing by 2π , we define the action function s , i.e., $s = \frac{1}{2\pi} \int_{\gamma} \alpha$. Its smoothness is checked as in Lemma 5.1. Let us describe the geometric meaning of the function s at $\Lambda < b$.

Recall that the action variable does not change when the cycle is replaced by a homologous cycle. Therefore, we consider as γ the cycle shown in Figure 16.1. Note that the standard projection π of this cycle onto the table touches the allowed velocity vector (on the layer) at each of its points. It follows that $s(\Lambda)$ is equal to the length of the curve $\pi(\gamma)$ (π is the standart projection on billiard table) multiplied by $\sqrt{2h}$. What happens to the curve $\pi(\gamma)$ when Λ goes to b ? This curve will become a four-linked broken line F_1PF_2Q , where F_1 and F_2 are the foci of the ellipse, and P and Q are two arbitrary points of the ellipse (see Fig. 16.2). By reason of the arbitrariness of P and Q we conclude that $|F_1P| + |PF_2| = \frac{1}{2\sqrt{2h}}s(b)$. In other words, we have arrived at the standard definition of an ellipse as the geometric place of points. The example may seem rather simple, nevertheless, using similar considerations, it is possible to prove Staudé's construction. Note that the authors previously proved Graves theorem on the construction of a confocal ellipse to a predetermined ellipse using a thread in a similar way (see [25]).

Now consider the ellipsoid given by the equation $\frac{x^2}{a^2} + \frac{y^2}{b^2} + \frac{z^2}{c^2} = 1$. As before, we assume that $a > b > c$. Consider the four-linked broken line FP_1PP_2G shown in Figure 4. We assume that P_1 and P_2 are chosen in such a way that all links

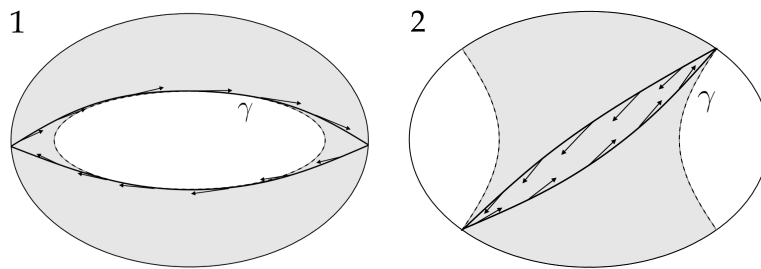


FIGURE 15. The cycle γ on Liouville tori close to the layer $\Lambda = b$, of billiard inside the ellipse: 1 — at $\Lambda < b$, 2 — at $\Lambda > b$.

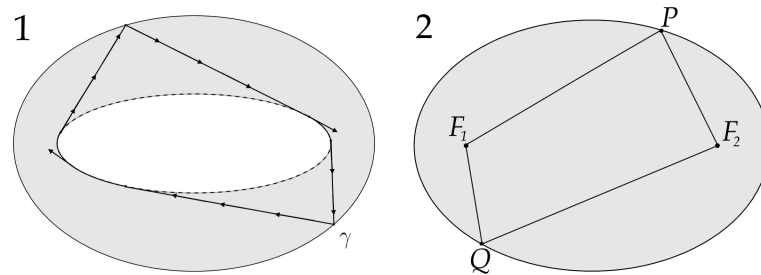


FIGURE 16. 1. The cycle γ on the Liouville torus represented as a stretched thread. 2. The projection on a billiard table of one of the limit positions of the cycle γ at $\Lambda \rightarrow b$.

of the broken line are sections of billiard trajectories passing through both focal curves, i.e., they lie at the isointegral level $\Lambda_1 = b$, $\Lambda_2 = c$. In this case, the broken line P_1PP_2 is an entire piece of the trajectory of the material point.

Note that when moving along the broken line FP_1PP_2G , each elliptic coordinate is passed exactly once (from the minimum to the maximum value and back again). Therefore, if we supplement this broken line with a symmetric piece (rotate it by π around the Ox axis), we obtain a cycle $\hat{\gamma}$ that goes around each elliptic coordinate exactly twice. However, this cycle will not, in general, be a cycle in Q_h^5 . Indeed, there is a break at the point P_1 . Therefore, to obtain a cycle on the layer $\Lambda_1 = b$, $\Lambda_2 = c$, it is necessary to lift $\hat{\gamma}$ on the layer, and then to connect by a continuous curve the ends of the lifts of the segments FP_1 and P_1P so that, when projected on the table, the connection segment coincides with the point P . Similarly, we should do the same with the point P_2 and the points symmetric to P_1 and P_2 . As a result, we get a cycle γ in Q_h^5 lying on the layer $\Lambda_1 = b$, $\Lambda_2 = c$. Since along this cycle each elliptic coordinate passes exactly twice, γ is homologous to the critical circle (see the beginning of the proof of the theorem 5.3), and hence the integral along γ of α is equal to the integral of the same form along the critical circle.

On the other hand, the integral $\int_\gamma \alpha$ is equal to twice the length of the broken line FP_1PPP_2G , since this broken line consists of two symmetric pieces, and all its segments are trajectory parts on the layer $\Lambda_1 = b$, $\Lambda_2 = c$. Thus, the length of the broken line FP_1PP_2G is constant. Moreover, it is equal to half of the integral of the form α along the critical circle divided by $\sqrt{2h}$. Easy calculations show that this number is equal to the major semi-axis multiplied by two, i.e., $2\sqrt{a}$.

If we imagine the broken line FP_1PP_2G as a thread of length $2\sqrt{a}$, it will be stretched in this position. This is ensured by the fact that the lines PP_1 and PP_2 pass through both focal curves.

Thus, if we want to construct an ellipsoid with semi-axes \sqrt{a} , \sqrt{b} , \sqrt{c} (or at least a part of it), we must choose a Cartesian coordinate system (x, y, z) and draw two focal curves: ellipse \mathfrak{F}_1 in the plane Oxy , given by the equation $\frac{x^2}{a-c} + \frac{y^2}{b-c} = 1$, and hyperbola \mathfrak{F}_2 in the plane Oxz , given by the equation $\frac{x^2}{a-b} - \frac{z^2}{b-c} = 1$. Next, we place movable joints on the focal ellipse \mathfrak{F}_1 and one of the branches of the focal hyperbola \mathfrak{F}_2 . Then, we take a thread of length \sqrt{a} , one end of which we pass through the joint at \mathfrak{F}_1 and connect to the focus of \mathfrak{F}_1 lying on the branch \mathfrak{F}_2 without the joint. We pass the other end of the thread through the second joint (i.e., at \mathfrak{F}_2) and connect it to the nearest focus of \mathfrak{F}_2 . The tension points of the thread will lie on the ellipsoid $\frac{x^2}{a} + \frac{y^2}{b} + \frac{z^2}{c} = 1$. Moreover, they will cover his quarter.

References

1. G. D. Birkhoff, *Dynamical systems*, AMS, New York, 1927.
2. V. V. Kozlov, D. V. Treshchev, *A Genetic Introduction to the Dynamics of Systems with Impact*, Transl. Math. Monogr. **89**, AMS, 1991.
3. S. Tabachnikov, *Geometria i billiardi*, NITs "Regulyarnaya i khaoticheskaya dinamika", Moscow – Izhevsk, 2011. Eng.: S. Tabachnikov, *Geometry and Billiards*, Stud. Math. Libr. **30**, AMS, Providence, RI, 2005.

4. V. Dragović, M. Radnović, *Bifurcations of Liouville tori in elliptical billiards*, Regul. Chaotic Dyn. **14**(4–5) (2009), 479–494.
5. V. Dragović, M. Radnović, *Integriruemye billiardy, kvadriki i mnogomernye porizmy Ponsele*, NITs “Regulyarnaya i khaoticheskaya dinamika”, Moscow–Izhevsk, 2010. Eng.: V. Dragovic, M. Radnovic, *Poncelet Porisms and Beyond*, Springer, Birkhauser, 2011.
6. V. V. Fokicheva, *Description of singularities for billiard systems bounded by confocal ellipses or hyperbolas*, Mosc. Univ. Math. Bull. **69**(4) (2014), 148–158.
7. V. V. Fokicheva, *Classification of billiard motions in domains bounded by confocal parabolas*, Sb. Math. **205**(8) (2014), 1201–1221.
8. V. V. Vedyushkina, I. S. Kharcheva, *Billiard books model all three-dimensional bifurcations of integrable Hamiltonian systems*, Sb. Math. **209**(12) (2018), 1690–1727.
9. V. V. Vedyushkina, I. S. Kharcheva, *Billiard books realize all bases of Liouville foliations of integrable Hamiltonian systems*, Sb. Math. **212**(8) (2021), 1122–1179.
10. I. F. Kobtsev, *The geodesic flow on a two-dimensional ellipsoid in the field of an elastic force. Topological classification of solutions*, Mosc. Univ. Math. Bull. **73**(2) (2018), 64–70.
11. I. F. Kobtsev, *An elliptic billiard in a potential force field: classification of motions, topological analysis*, Sb. Math. **211**(7) (2020), 987–1013.
12. S. E. Pustovoytov, *Topological analysis of a billiard in elliptic ring in a potential field*, J. Math. Sci. **259**(5) (2021), 712–729.
13. S. E. Pustovoitov, *Topological analysis of a billiard bounded by confocal quadrics in a potential field*, Sb. Math. **212**(2) (2021), 211–233.
14. V. Dragović, M. Radnović, *Topological invariants for elliptical billiards and geodesics on ellipsoids in the Minkowski space*, J. Math. Sci. **223**(6) (2017), 686–694.
15. E. E. Karginova, *Billiards bounded by arcs of confocal quadrics on the Minkowski plane*, Sb. Math. **211**(1) (2020), 1–28.
16. V. V. Vedyushkina, V. N. Zav’yalov, *Realization of geodesic flows with a linear first integral by billiards with slipping*, Sb. Math. **213**(12) (2022), 1645–1664.
17. V. V. Vedyushkina, A. T. Fomenko, *Force evolutionary billiards and billiard equivalence of the Euler and Lagrange cases*, Dokl. Math. **103**(1) (2021), 1–4.
18. A. T. Fomenko, V. V. Vedyushkina, *Evolutionary force billiards*, Izv. Math. **86**(5) (2022), 943–979.
19. G. V. Belozеров, *Topological classification of integrable geodesic billiards on quadrics in three-dimensional Euclidean space*, Sb. Math. **211**(11) (2020), 1503–1538.
20. A. T. Fomenko, *Topological invariants of Liouville integrable Hamiltonian systems*, Funct. Anal. Appl. **22**(4) (1988), 286–296.
21. A. T. Fomenko, *The symplectic topology of completely integrable Hamiltonian systems*, Russ. Math. Surv. **44**(1) (1989), 181–219.
22. A. V. Bolsinov, S. V. Matveev, A. T. Fomenko, *Topological classification of integrable Hamiltonian systems with two degrees of freedom. List of systems of small complexity*, Russ. Math. Surv. **45**(2) (1990), 59–94.
23. A. T. Fomenko, H. Zieschang, *A topological invariant and a criterion for the equivalence of integrable Hamiltonian systems with two degrees of freedom*, Math. USSR, Izv. **36**(3) (1991), 567–596.
24. G. V. Belozеров, *Topological classification of billiards bounded by confocal quadrics in three-dimensional Euclidean space*, Sb. Math. **213**(2) (2022), 129–160.
25. G. V. Belozеров, A. T. Fomenko, *Orbital invariants of billiards and linearly integrable geodesic flows*, Sb. Math. **215**(5) (2024), 573–611.
26. D. Hilbert, S. Cohn-Vossen, *Anschauliche Geometrie*, Springer-Verlag Berlin Heidelberg, 1932; D. Hilbert, S. Cohn-Vossen, *Geometry and the imagination* (2nd ed.), AMS Chelsea Pub., Providence, R.I., 1999.
27. G. V. Belozеров, *Topology of 5-surfaces of a 3D billiard inside a triaxial ellipsoid with Hooke’s potential*, Mosc. Univ. Math. Bull. **77**(6) (2022), 277–289.

28. K. Yakobi, *Lektsii po dinamike*, Gostekhizdat, Moscow, 1936; Orig.: C. Jacobi, *Vorlesungen über dynamik*, 1865; Eng.: *Jacobi's Lectures on Dynamics*, Texts Read. Math. **51**, Springer, 2009.
29. M. Chasles, *Sur les lignes géodésiques et les lignes de courbure des surfaces du second degré*, Journal de Mathématiques Pures et Appliquées **11** (1846), 5–20.
30. V. I. Arnold, *Mathematical Methods of Classical Mechanics*, Grad. Texts Math. **60**, Springer-Verlag, 1989.
31. V. Dragović, B. Gajić, *Points with rotational ellipsoids of inertia, envelopes of hyperplanes which equally fit the system of points in R^k , and ellipsoidal billiards*, Physica D **451**(15) (2023), 133776.
32. V. Dragović, B. Gajić, *Orthogonal and Linear Regressions and Pencils of Confocal Quadrics*, Stat. Sci. **40**(2) (2025), 289–312.
33. V. Dragovic, M. Radnovic, *Geometry of integrable billiards and pencils of quadrics*, J. Math. Pures Appl. (9) **85**(6) (2006), 758–790.
34. S-J. Chang, R. Friedberg, *Elliptical billiards and Poncelet's theorem*, J. Math. Phys. **29**(7) (1988), 1537–1550.
35. B. Crespi, S-J. Chang, K. J. Shi, *Elliptical billiards and hyperelliptic functions*, J. Math. Phys. **34**(6) (1993), 2257–2289.
36. J. Moser, A. P. Veselov, *Discrete versions of some classical integrable systems and factorization of matrix polynomials*, Comm. Math. Phys. **139**(2) (1991), 217–243.
37. T. Z. Nguen, *Symplectic topology of integrable Hamiltonian systems, I: Arnold–Liouville with singularities*, Compos. Math. **101** (1996), 179–215.
38. A. V. Bolsinov, A. T. Fomenko, *Integrable Hamiltonian systems. Geometry, topology, classification*, Chapman & Hall/CRC, Boca Raton, FL, 2004.
39. V. V. Vedyushkina, V. A. Kibkalo, S. E. Pustovoitov, *Realization of focal singularities of integrable systems using billiard books with a Hooke potential field*, Chebyshevskii Sb. **22**(5) (2021), 44–57.
40. V. Lazutkin, *KAM Theory and Semiclassical Approximations to Eigenfunctions*, Springer-Verlag, Berlin, 1993.
41. E. A. Kudryavtseva, *Liouville integrable generalized billiard flows and Poncelet type theorems*, J. Math. Sci., New York **225**(4) (2017), 611–638.
42. A. V. Bolsinov, P. H. Richter, A. T. Fomenko, *The method of loop molecules and the topology of the Kovalevskaya top*, Sb. Math. **191**(2) (2000), 151–188.
43. A. T. Fomenko, V. A. Kibkalo, *Saddle singularities in integrable Hamiltonian systems: Examples and algorithms*, In: V. A. Sadovnichiy, M. Z. Zgurovsky (eds.), *Contemporary Approaches and Methods in Fundamental Mathematics and Mechanics*, Understanding Complex Systems, Springer, Cham, 2021, 3–26.

**СИНГУЛАРИТЕТИ ТРОДИМЕНЗИОНИХ БИЛИЈАРА
ОГРАНИЧЕНИХ КОНФОКАЛНИМ КВАДРИКАМА**

РЕЗИМЕ. Разматран је проблем кретања материјалне тачке у тродимензионалном домену ограниченом конфокалним квадрикама. Такав динамички систем је Лиувил интегрabilан у део-по део глатком смислу. За два типа билијаских домена, пронађени су региони могућег кретања материјалне тачке, конструисани су бифуркациони дијаграми и описана је полулокална структура Лиувилове фолијације. На сингуларним слојевима Лиувилове фолијације различитог ранга, барем једна променљива дејства може се глатко проширити. Ово разматрање, примењено на билијар унутар троосног елипсоида, даје нови доказ Штаудеове конструкције елипсоида коришћењем нити.

Department of Differential Geometry and Applications
Faculty of Mechanics and Mathematics
Lomonosov Moscow State University
Moscow
Russia
g1eb0511beloz@yandex.ru
<https://orcid.org/0009-0004-9343-1949>

(Received 22.01.2025)
(Revised 19.11.2025)
(Available online 22.12.2025)

Department of Differential Geometry and Applications
Faculty of Mechanics and Mathematics
Lomonosov Moscow State University
Moscow
Russia
atfomenko@mail.ru